

Electronic Supplementary Information

Sulfoxide Hemithioindigo Tweezers – Visible Light Addressable Capture and Release

Thomas Bartelmann,[†] Frederik Gnannt,[§] Max Zitzmann,[§] Peter Mayer,[†] Henry Dube^{†§*}

[†] Ludwig-Maximilians-Universität München, Department of Chemistry and Center for Integrated Protein Science CIPSM, Butenandtstr. 5-13, 81377 München

[§] Friedrich-Alexander-Universität Erlangen-Nürnberg, Department of Chemistry and Pharmacy, Nikolaus-Fiebiger-Str. 10, 91058 Erlangen

* E-mail: henry.dube@fau.de

Table of Contents

General experimental	2
Synthesis	4
(Z)-7-(3',5'-dimethoxy-3,5-dimethyl-[1,1'-biphenyl]-4-yl)-2-(6-(3',5'-dimethoxy-3,5-dimethyl-[1,1'-biphenyl]-4-yl)-2,2-dimethyl-2,3-dihydro-1H-inden-1-ylidene)benzo[b]thiophen-3(2H)-one 1-oxide (4)	4
Photophysical properties of 4.....	6
Photoisomerization of 4 under continuous irradiation	6
Molar absorption coefficients of 4	8
Photophysical properties of 4·5.....	11
Thermal stability of the isomers of 4	12
Binding properties of the isomers of 4 with guest molecule 5	14
Van't Hoff analysis	21
Binding affinities between tweezers Z-3 and Z-4 and guest molecules 6 - 8	26
Summary of the binding parameters for complexes of Z-4 with guest molecules 5 - 8 ..	57
Theoretical description of 4 and the Z-4·5 complex	58
NMR spectra	60
¹ H and ¹³ C NMR spectra of 4.....	60
Crystal structural data	61
Calculated ground state minima geometries - xyz coordinates	63
References.....	69

General experimental

Reagents and solvents

Reagents and dry solvents were used as received without further purification. Technical solvents were distilled (rotary evaporator *vacuubrand CVC 3000*) before use for column chromatography and extraction. Thin layer chromatography was performed on *Merck Silica F254 TLC* plates. Detection was done by UV light (254 nm and 366 nm) or cerium ammonium molybdate staining.

Guest compounds

1,2,4,5-Tetracyanobenzene (TCNB) **6** and 4-Nitrophthalic anhydride (PhA) **7** were purchased from *Sigma Aldrich*. 3-Nitrophthalonitrile (3NPN) **8** was purchased from *TCI Germany*. All compounds were used as received without further purification.

Column chromatography

Column chromatography was performed with silica gel 60 (*Merck*, particle size 0.063 – 0.200 mm) and technical distilled solvents.

High performance liquid chromatography

HPLC was performed on a *Shimadzu* HPLC system with a LC-20AP solvent delivery module, a CTO-20A column oven, a SPD-M20A photodiode array UV-Vis detector and a CBM-20A system controller. HPLC solvents (*n*-heptane and EtOAc) were purchased from *VWR International*, *Alfa Aesar* and *Fisher Scientific*. As stationary phase a preparative *NUCLEODUR*® 100-5 column (particle size 5 µm), a semipreparative *CHIRALPAK*® IC column (particle size 5 µm), and a semipreparative *CHIRALPAK*® ID column (particle size 5 µm) were used.

Medium pressure liquid chromatography

MPLC was performed on a *Biotage Isolera One*. As stationary phase a *CHROMABOND*® Flash RS 25 SiOH column (particle size 40-63 µm) was used.

¹H and ¹³C NMR spectroscopy

NMR spectra were recorded on a *Varian Mercury 200 VX*, *Varian 300*, *Inova 400*, *Varian 600 NMR*, *Bruker Avance 400 MHz*, or *Bruker Avance III HD 800 MHz* spectrometer. Deuterated solvents were purchased from *Eurisotop*, *Deutero*, and *Sigma Aldrich*. Chemical shifts (δ) are reported relative to tetramethylsilane. Solvent signals were used as internal standard in the ¹H and ¹³C NMR spectra. For ¹H NMR: CDCl₃ = 7.26 ppm, CD₂Cl₂ = 5.32 ppm, acetone-*d*₆ = 2.05 ppm, DMSO-*d*₆ = 2.50 ppm. For ¹³C NMR: CDCl₃ = 77.16 ppm, CD₂Cl₂ =

53.84 ppm, acetone- d_6 = 206.68, 29.92 ppm, DMSO- d_6 = 39.52 ppm. The resonance multiplicity is indicated as *s* (singlet), *d* (doublet), *t* (triplet), *q* (quartet), *m* (multiplet), and *br* (broad signal). The chemical shifts are given in parts per million (ppm) on the delta scale (δ), and the coupling constant values (*J*) are given in hertz (Hz).

Mass spectrometry

Electron impact (EI) mass spectrometry was performed on a *Finnigan MAT95Q* or on a *Finnigan MAT90* mass spectrometer. Electrospray ionisation (ESI) mass spectra were measured on a *Thermo Finnigan LTQ-FT*. Signals are reported in *m/z* units.

Infrared spectroscopy

IR spectra were recorded on a *Perkin Elmer Spectrum BX-FT-IR* spectrometer equipped with a *Smith DuraSamplIR II ATR* accessory. Transmittance values are given qualitatively by wavenumber and intensity (very strong (vs), strong (s), medium (m), and weak (w)).

UV/Vis spectroscopy

UV/VIS spectra were recorded on a *Varian Cary 5000* spectrophotometer in 1 cm quartz cuvettes. Solvents for UV/Vis spectroscopy were purchased from *VWR International* and used as received. Absorption wavelengths at maxima (λ_{max}) are reported in nm and the molar absorption coefficients (ϵ) $L \cdot mol^{-1} \cdot cm^{-1}$ subsequently in brackets. Shoulders are declared as sh.

Melting points

(M.p.) were measured on a *Büchi B-540* melting point apparatus in open capillaries.

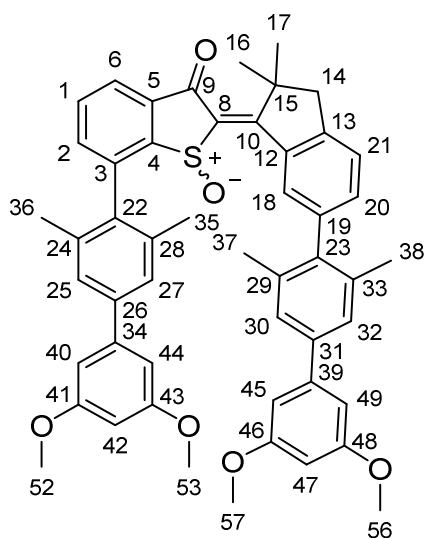
Irradiation experiments (LEDs)

LEDs for irradiation experiments were purchased from *Roithner Lasertechnik GmbH* (365 nm, 405 nm, 430 nm, 470 nm, 530 nm).

Synthesis

The precursors of **4** and **5** were synthesized according to previously reported procedures.¹

(Z)-7-(3',5'-dimethoxy-3,5-dimethyl-[1,1'-biphenyl]-4-yl)-2-(6-(3',5'-dimethoxy-3,5-dimethyl-[1,1'-biphenyl]-4-yl)-2,2-dimethyl-2,3-dihydro-1H-inden-1-ylidene)benzo[b]thiophen-3(2H)-one 1-oxide (**4**)



Tweezers **3** (1.0 equiv., 250 mg, 0.323 mmol) and $\text{NaBO}_3 \cdot 4 \text{H}_2\text{O}$ were dissolved in 5.0 mL acetic acid and stirred for 20 h at 22 °C. The reaction mixture was quenched with a saturated aqueous NaHCO_3 solution (20 mL) and extracted with EtOAc (3×100 mL). The combined organic phases were dried over MgSO_4 . The solvent was removed *in vacuo* and the crude product was purified by MPLC (SiO_2 , *i*Hex \rightarrow *i*Hex:EtOAc 1:1) and normal phase HPLC (*i*Hex:EtOAc 80:20). Compound **4** (246 mg, 96%) was received as a light-yellow solid.

R_f (SiO_2 , *i*Hex:EtOAc = 85:15) = 0.07, m.p.: 157-163 °C.

Z-isomer:

$^1\text{H-NMR}$ (599 MHz, CDCl_3) δ = 8.19 (d, 4J = 1.4 Hz, 1H, H-C(18)), 8.03 (dd, 3J = 7.7, 4J = 1.1 Hz, 1H, H-C(6)), 7.81 (t, 3J = 7.5 Hz, 1H, H-C(1)), 7.54 (dd, 3J = 7.4, 4J = 1.2 Hz, 1H, H-C(2)), 7.38 (d, 3J = 7.8 Hz, 1H, H-C(21)), 7.34 (s, 1H, H-C(25 or 27)), 7.33 (s, 1H, H-C(25 or 27)), 7.28 (dd, 3J = 7.6, 4J = 1.4 Hz, 1H, H-C(20)), 7.24 (s, 1H, H-C(30 or 32)), 7.20 (s, 1H, H-C(30 or 32)), 6.77 (d, 4J = 2.3 Hz, 2H, H-C(40,44)), 6.69 (d, 4J = 2.2 Hz, 2H, H-C(45, 49)), 6.47 (t, 4J = 2.2, 1.8 Hz, 1H, H-C(47)), 6.46 (t, 4J = 1.8 Hz, 1H, H-C(42)), 3.84 (s, 6H,

H-C(56,57)), 3.79 (s, 6H, H-C(52,53)), 3.15 (s, 2H, H-C(14)), 2.11 (s, 3H, H-C(35 or 36)), 2.06 (s, 3H, H-C(37 or 38)), 2.04 (s, 3H, H-C(35 or 36)), 2.03 (s, 3H, H-C(37 or 38)), 1.74 (s, 3H, H-C(16 or 17)), 1.64 (s, 3H, H-C(16 or 17)). ^{13}C NMR (151 MHz, CDCl_3) δ = 187.2 (C(9)), 177.2 (C(10)), 161.1 (C(46,48)), 161.1 (C(41,43)), 149.5 (C(13)), 147.2 (C(4)), 143.5 (C(34)), 143.5 (C(39)), 141.6 (C(26)), 141.5 (C(5)), 140.4 (C(31)), 140.2 (C(19)), 140.1 (C(12)), 138.5 (C(24 or 28)), 138.0 (C(23)), 137.3 (C(29 or 33)), 136.7 (C(29 or 33)), 136.5 (C(8)), 136.4 (C(2)), 136.2 (C(3)), 135.9 (C(24 or 28)), 135.3 (C(22)), 135.1 (C(20)), 133.4 (C(1)), 130.7 (C(18)), 126.9 (C(25 or 27)), 126.7 (C(30 or 32)), 126.5 (C(30 or 32)), 126.3 (C(25 or 27)), 125.4 (C(21)), 125.0 (C(6)), 105.5 (C(40, 44)), 105.5 (C(45,49)), 99.7 (C(42)), 99.6 (C(47)), 55.6 (C(56,57)), 55.5 (C(52,53)), 50.8 (C(14)), 49.8 (C(15)), 26.7 (C(16 or 17)), 26.4 (C(16 or 17)), 21.6 (C(35 or 36)), 21.4 (C(37 or 38)), 21.3 (C(35 or 36)), 21.1 (C(37 or 38)). IR: $\tilde{\nu}$ = 2927w, 1679m, 1595s, 1569m, 1533m, 1457m, 1428m, 1387w, 1354w, 1268m, 1203s, 1153vs, 1103w, 1066s, 983w, 941w, 927w, 875w, 828s, 763m, 717w, 693w. UV/Vis (CHCl_3): λ_{max} (ϵ) = 266 nm (43,482), 371 nm (15,396).

E-isomer:

^1H -NMR (800 MHz, CDCl_3): δ = 8.30 (s, 1H, C-H(18)), 8.02 (dd, 3J = 7.7, 1.1 Hz, 1H, C-H(6)), 7.83 (t, 3J = 7.5 Hz, 1H, C-H(1)), 7.57 (dd, 3J = 7.3, 1.2 Hz, 1H, C-H(2)), 7.45 – 7.39 (m, 4H, C-H(25,27,30,32)), 7.35 (d, 3J = 1.9 Hz, 1H, C-H(21)), 7.30 (d, 3J = 7.5 Hz, 1H, C-H(20)), 6.83 (d, 3J = 2.2 Hz, 2H, C-H(40,44)), 6.81 (d, 3J = 2.2 Hz, 2H, C-H(45,49)), 6.51 (t, 3J = 2.3 Hz, 2H, C-H(42,47)), 3.90 (s, 12H, C-H(52,53,57,56)), 3.29 (d, 3J = 15.3 Hz, 1H, C-H₂(14)), 2.93 (d, 3J (H,H) = 15.3 Hz, 1H, C-H(14)), 2.35 (s, 3H, C-H(35)), 2.19 (s, 3H, C-H(36)), 2.09 (s, 3H, C-H(37 oder 38)), 2.07 (s, 3H, C-H(37 oder 38)), 1.89 (s, 3H, C-H(16 oder 17)), 1.52 (s, 3H, C-H₃(16 oder 17)) ppm.

IR: $\tilde{\nu}$ = 2954w, 1676m, 1594s, 1569m, 1533m, 1457m, 1388w, 1347w, 1268s, 1203s, 1153vs, 1099w, 1058s, 927w, 875w, 829s, 768m, 747w, 693m, 658w. UV-Vis (CHCl_3): λ_{max} (ϵ) = 264 (45,808), 360 (14,476), 379 nm(13,664).

HR-EI-MS calcd. [$\text{C}_{51}\text{H}_{48}\text{O}_6\text{S}$]: 788.3172, found: 788.3166.

Photophysical properties of **4**

Photoisomerization of **4** under continuous irradiation

For quantitative analysis of the isomer composition in the photostationary state (PSS) of **4**, obtained under continuous irradiation at a given wavelength, an NMR tube was charged with a 15 mM solution of **4** in CDCl₃. Light with the wavelength of 365 nm and 405 nm was used for the *Z* to *E* photoisomerization and light of 470 nm for the *E* to *Z* photoisomerization. Irradiation of the NMR tubes was conducted using medium power (about 100-300 mW output) LEDs outside the NMR spectrometer. After different time intervals of irradiation ¹H-NMR spectra were recorded to monitor the photoisomerization progress. The isomeric composition was determined by integration of the proton 18 signals, which are significantly different for the *E* and *Z* isomers of **4**. Irradiation was stopped when no further changes in the isomeric composition were observable. At the high 15 mM sample concentration and the medium irradiation power, the *E* isomer proportion reached 83% after 60 min irradiation with light of 365 nm wavelength. The *Z* isomer proportion reached 75% after 225 min irradiation with light of 470 nm wavelength.

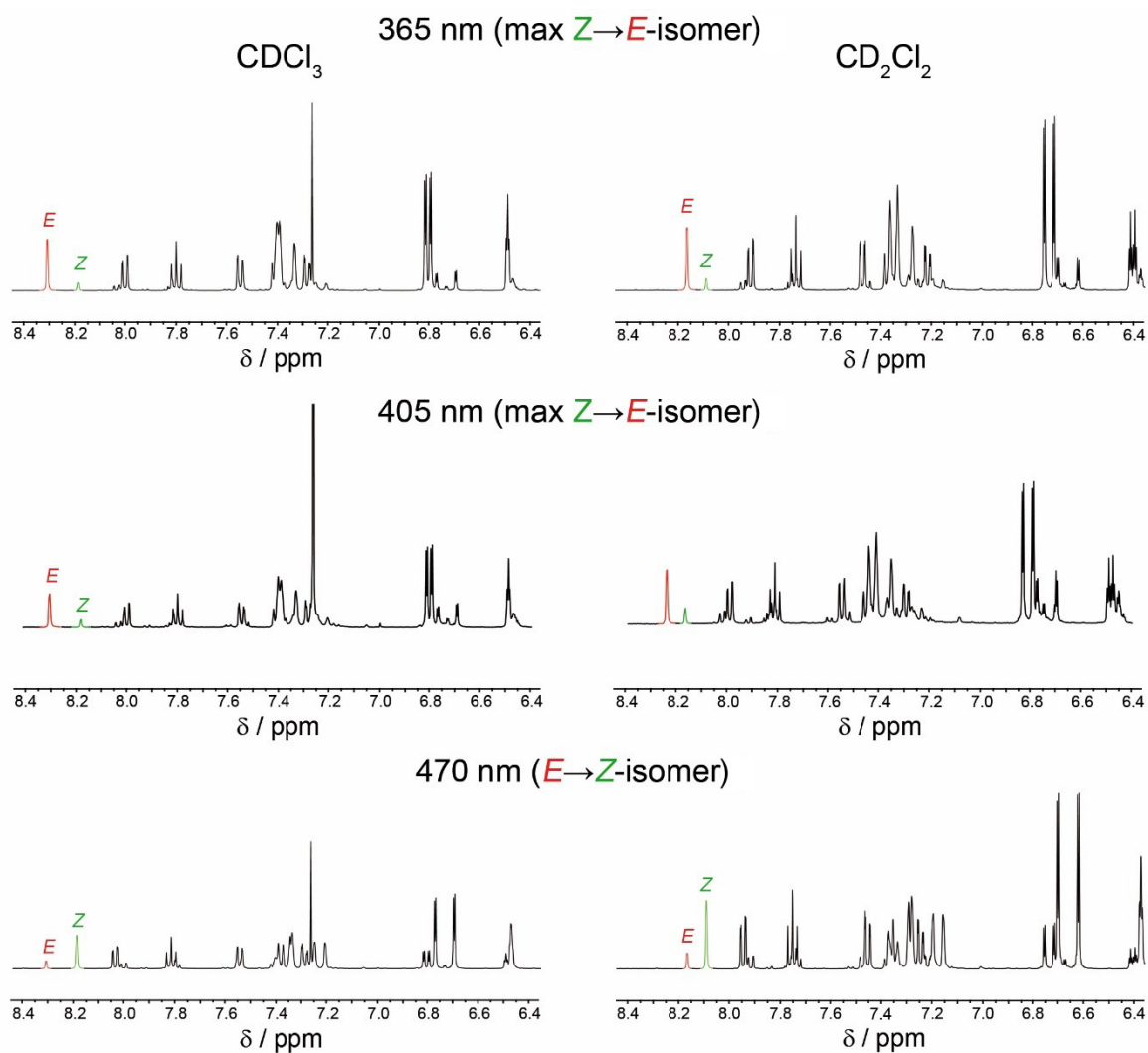


Figure S1: NMR analysis of the photoisomerization of **4** in solution. Aromatic sections of ^1H -NMR spectra (400 MHz, 293 K, left: CDCl_3 , right: CD_2Cl_2) recorded at the PSS at 365 nm irradiation (top) and at 470 nm irradiation (bottom). Signals of proton 18 used for determination of the isomeric ratio are indicated by color (*E* in red, *Z* in green).

Table S1: Isomeric composition of **4** (in CDCl_3 (15 mM) and CD_2Cl_2) obtained in the PSS at 365 nm, 405 nm, and 470 nm irradiation. Isomer yields were determined by ^1H -NMR spectroscopy and integration of the respective *E* and *Z* isomer signals of proton 18.

Solvent	% <i>E</i> -isomer (365 nm)	% <i>E</i> -isomer (405 nm)	% <i>Z</i> -isomer (470 nm)
CDCl_3	88	83	80
CD_2Cl_2	83	78	83

Molar absorption coefficients of **4**

For the determination of the molar absorption coefficients of **4** a defined amount of a *E/Z* isomer mixture was dissolved in a defined volume (volumetric flask) of the respective solvent (Table S2).

Table S2: Prepared solutions for the determination of the extinction coefficients of **4** in CHCl₃ and CH₂Cl₂.

solvent	<i>m</i> [mg]	<i>V</i> [mL]	<i>c</i> [μmol L ⁻¹]
CHCl ₃	0.6824	10	86
CH ₂ Cl ₂	0.2705	5	69

UV/Vis spectra of the resulting solutions were recorded. In order to determine the isosbestic points additional UV/Vis spectra were recorded after irradiation with light of 365 nm wavelength. To obtain UV/Vis spectra of pure isomers, an *E/Z* isomeric mixture of **4** was separated by HPLC into the pure *E* and *Z* isomers. Each isomer was subsequently dissolved in the respective chlorinated solvent in an undefined concentration and a UV/Vis spectrum was recorded. Then the spectra of the pure isomers were scaled with an upkeep factor to match the isosbestic points determined before quantitatively. Molar absorption coefficients were calculated by equation 1.

$$\varepsilon = \frac{A}{c \cdot d} \quad (\text{eq. 1})$$

with ε = molar extinction coefficient

A = Absorption

c = molar concentration

d = path length

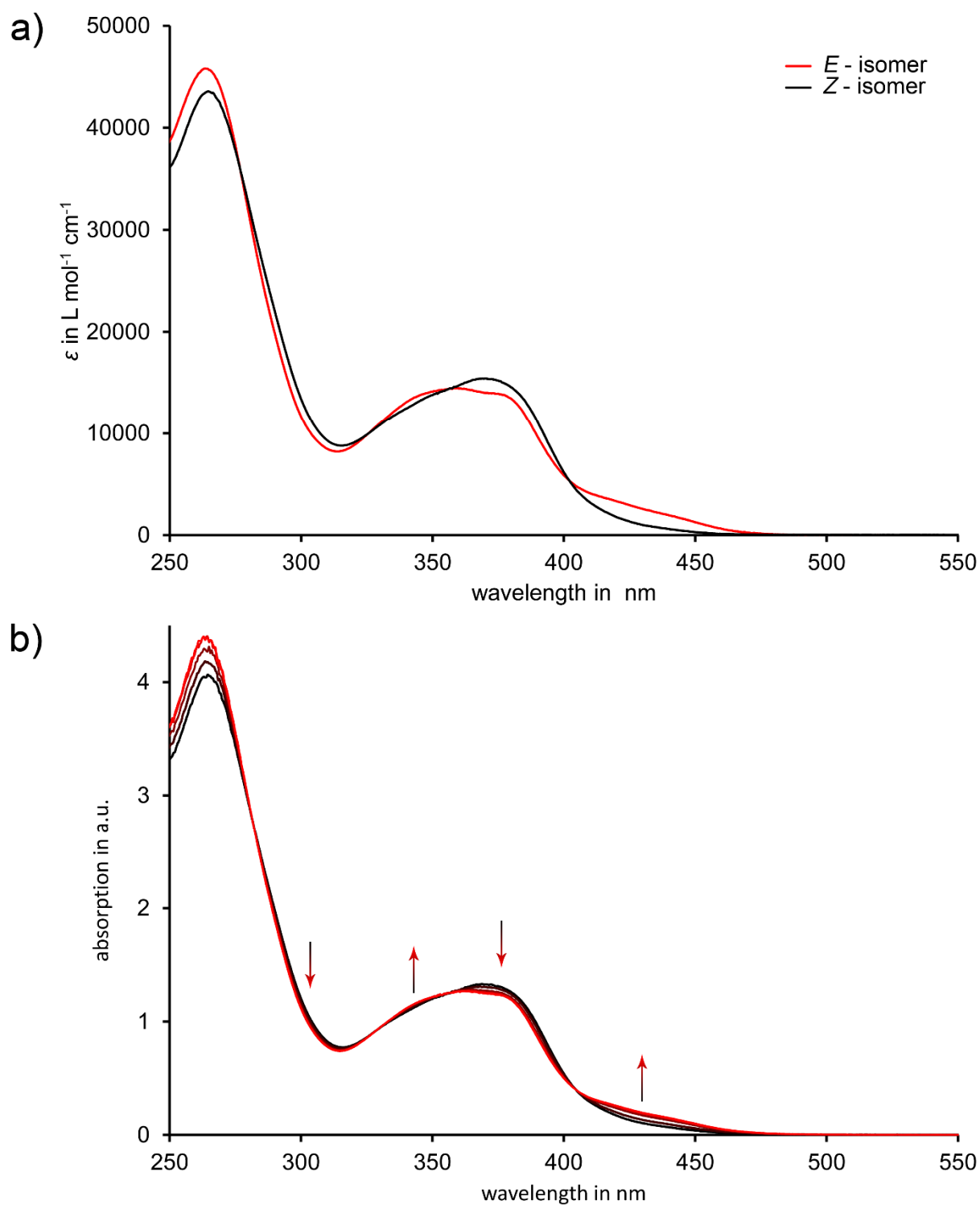


Figure S2: Molar absorption coefficients of **4** and UV/Vis spectral changes upon photoisomerization in CHCl₃. a) Molar absorption coefficients of **4** in CHCl₃. b) Spectral changes observed during *Z* to *E* photoisomerization after irradiation with light of 365 nm wavelength. Arrows indicate increasing and decreasing absorptions. Isosbestic points are observed at 282 nm, 328 nm, 357 nm, and 405 nm.

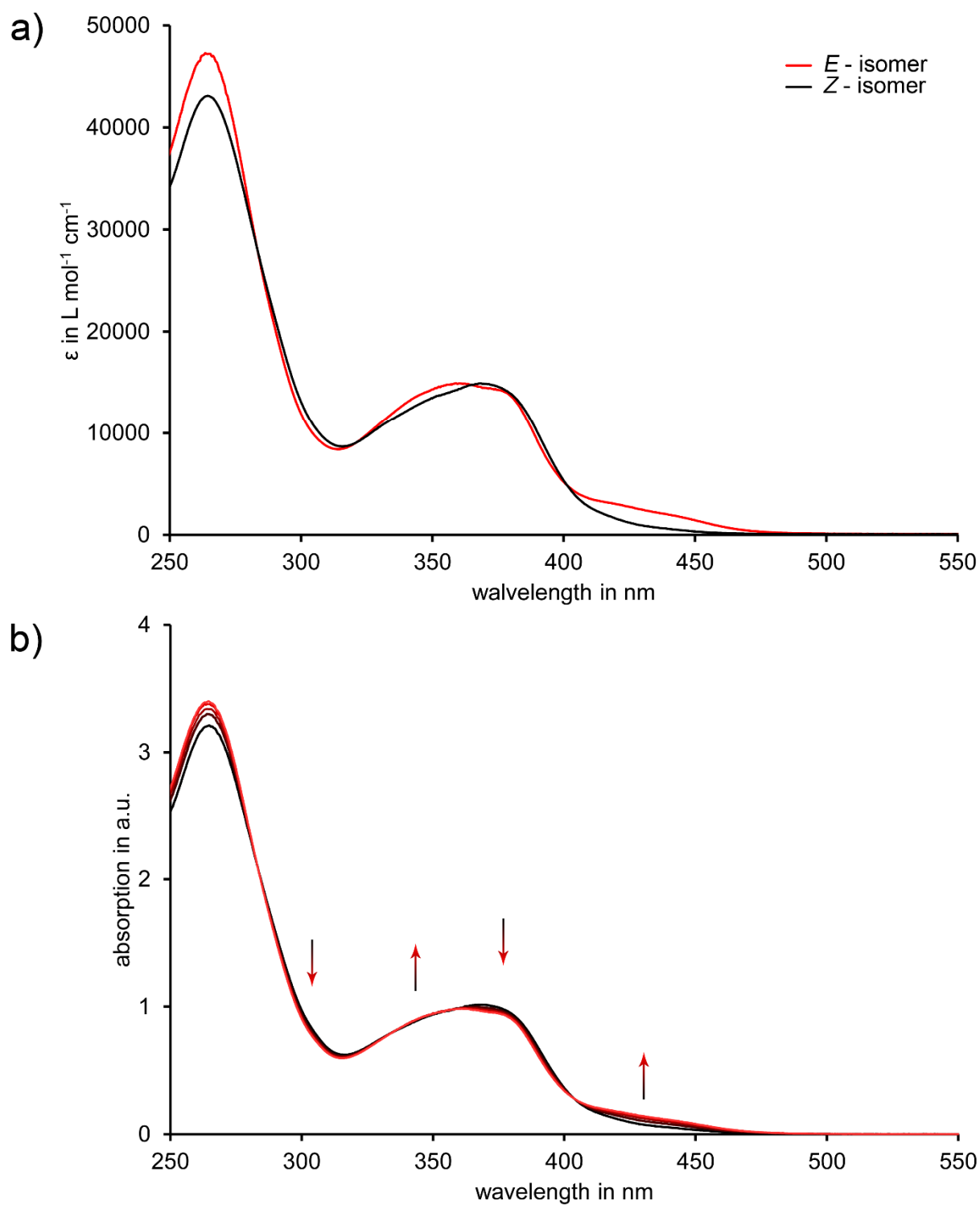


Figure S3: Molar absorption coefficients of **4** and UV/Vis spectral changes upon photoisomerization in CH_2Cl_2 . a) Molar absorption coefficients of **4** in CH_2Cl_2 . b) Spectral changes observed during *Z* to *E* photoisomerization after irradiation with light of 365 nm wavelength. Arrows indicate increasing and decreasing absorptions. Isosbestic points are observed at 283 nm, 335 nm, 358 nm, and 403 nm.

Photophysical properties of 4·5

In order to determine the photophysical properties of the 4·5 association complex, guest molecule 5 was dissolved in an 86 μM solution of 4 in CHCl_3 . The resulting ratio between 4 and 5 was 1:10. New broad spectral features (charge transfer (CT) band) in the range between 500 and 560 nm arise upon formation of the association complex 4·5. The CT band is photoswitchable with light of the same wavelengths as used for photoisomerization of the pure tweezers 4. As a result of photoisomerization a decreasing CT band is observed after irradiating with light of 365 nm.

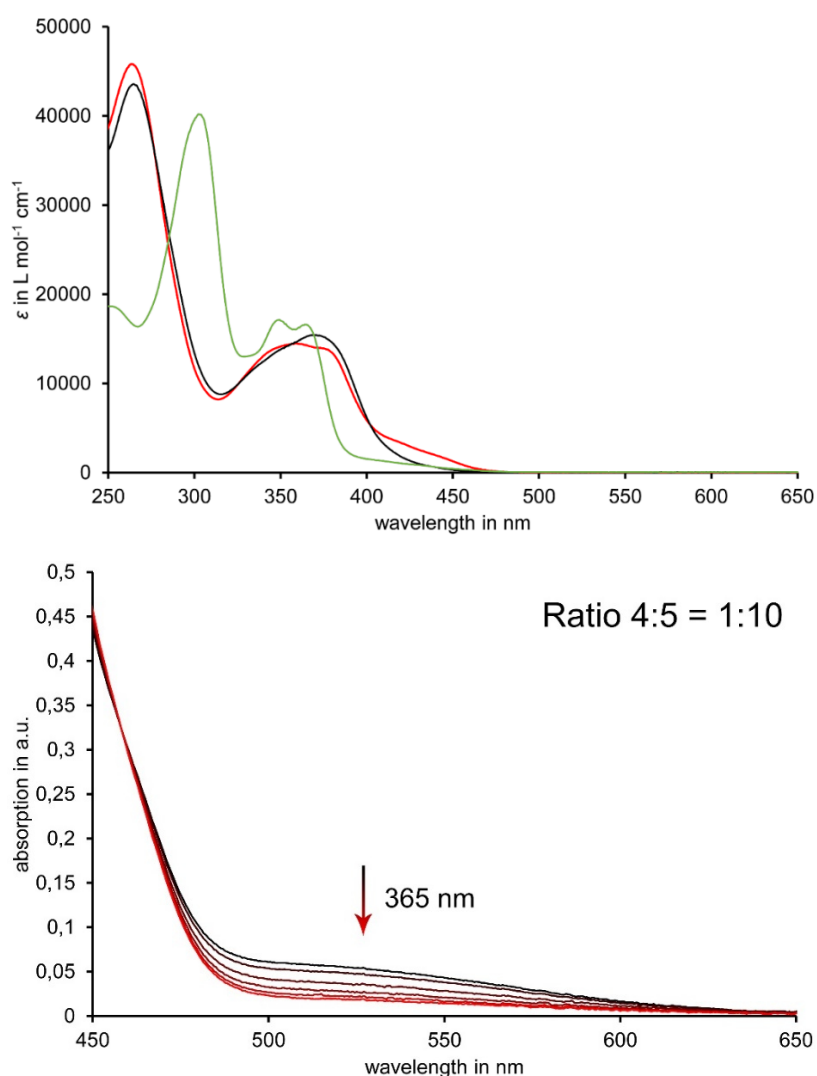


Figure S4: UV/vis spectral changes observed upon addition of guest 5 to a CHCl_3 solution of 4 (20 °C). a) Full UV/vis spectra of pure Z-4 (black), pure E-4 (red), and of the 1:10 mixture of 4·5 (green). b) Photoswitchable CT band observed at longer wavelengths after adding a 10fold excess of 5 to 4.

Thermal stability of the isomers of **4**

For the elucidation of the thermal stability of the isomers of **4**, pure *E*-**4** was dissolved in toluene-*d*₈ and heated at 100 °C for 27 h. In defined time intervals ¹H-NMR spectra were recorded and the isomeric ratio was determined by integration and comparing of the indicative proton 18 signals. Since there was no change visible in the isomeric ratio, the solution was irradiated with light of 470 nm wavelength to generate a different isomeric ratio. This solution was heated again at 100 °C for 10 h. This experiment was done to ensure that the solution was not already thermally equilibrated. No change of the isomeric ratio upon heating at 100 °C was visible in this case again.

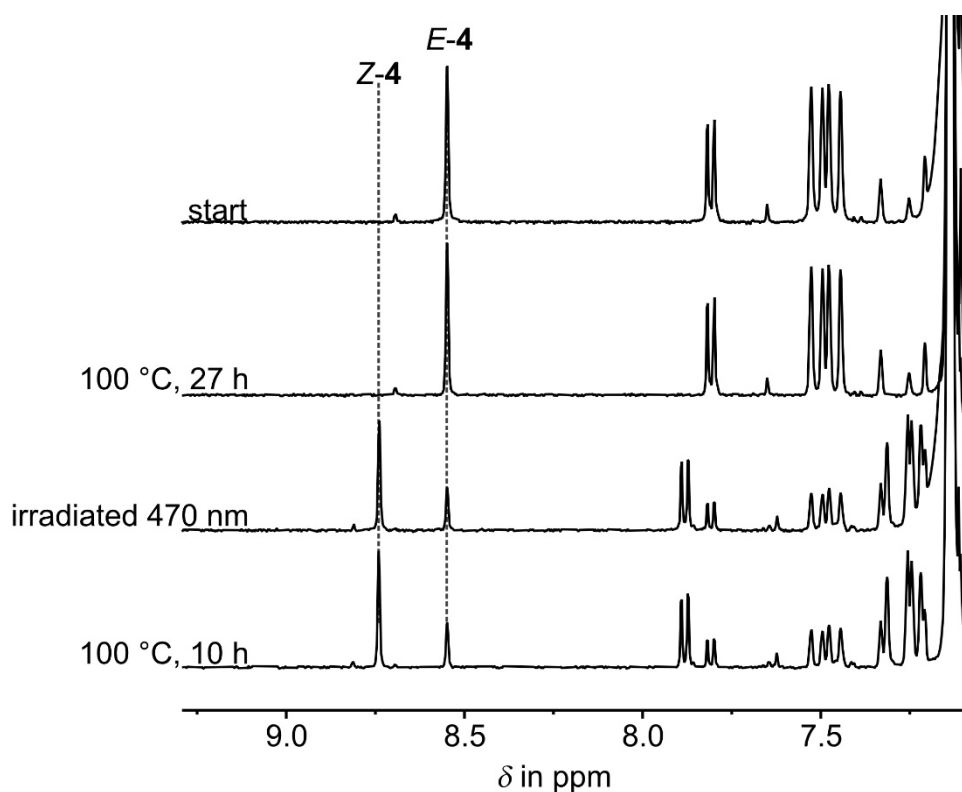


Figure S5: Testing of the thermal stability of individual isomers of **4** in solution. Aromatic section of the ¹H-NMR spectra (400 MHz, 293 K, CDCl₃) of **4** recorded to elucidate the energy barrier of the thermal *E* to *Z* or *Z* to *E* isomerizations. Different *E*/*Z* isomer mixtures were heated at 100 °C for 27 h and 10 h showing no visible changes of the isomeric ratio.

Conservatively assuming that 5% changes in isomer composition is not detectable by the NMR spectrometer – i.e. that 5% *Z*-isomer was accumulated at 100 °C after 27 h – a rate constant of $k = 5.13 \cdot 10^{-7} \text{s}^{-1}$ can be calculated. To this end it also has to be assumed that in thermal

equilibrium only the *Z* isomers is populated. According to the *Eyring* equation (eq. 2) this translates to a barrier $\Delta G^\ddagger > 33.0 \text{ kcal}\cdot\text{mol}^{-1}$.

$$k = \frac{k_B T}{h} e^{\frac{-\Delta G^\ddagger}{RT}} \quad (\text{eq. 2})$$

with $k_B = \text{Boltzmann constant } (1.381 \cdot 10^{-23} \text{ J}\cdot\text{K}^{-1})$

$T = \text{temperature in K}$

$h = \text{Planck constant } (6.626 \cdot 10^{-34} \text{ J}\cdot\text{s})$

Binding properties of the isomers of **4** with guest molecule **5**

When examining spectral changes upon addition of guest molecule **5** to solutions of **4** only signals of the closed tweezers form *Z-4* were shifted. Signals of the open tweezers form *E-4* remained unchanged. When mixing pure *E-4* and **5** also the signals of guest **5** remained unchanged. These experiments give clear evidence that only *Z-4* possesses affinity for guest **5** and no binding occurs for the open form of tweezers **4**. As a result a high modulation of binding and efficient guest release is possible with tweezers **4**.

For the determination of the binding constant (K_a) of *Z-4* and **5** a titration experiment was performed. Since there are no signs of interaction between the open form *E-4* and **5**, a new titration method with the aid of light was conducted. Excess of tweezers **4** was used because of the limited solubility of **5** in CDCl_3 .

Therefore, a solution of **5** (0.4018 mg in 4 ml CDCl_3) was split and 1.5 mL of this solution was added to solid tweezers (*solution 1*: 0.6844 mg covering the range from 0.25 equiv. to 1.6 equiv. of tweezers **4**; *solution 2*: 5.1769 mg, covering the range from 1.9 equiv. to 12.7 equiv. of tweezers **4**). These solutions were transferred into two respective NMR tubes and $^1\text{H-NMR}$ spectra were recorded. Multiple titration points were measured ($^1\text{H-NMR}$ spectra) by consecutive irradiation with light of 365 nm or 470 nm wavelength, changing the ratio of guest to tweezers. The specific ratio was determined each time by integration and comparison of guest signal **c** (with constant integral because of the constant concentration of **5**) with the integrated signal of proton 18 of *Z-4*. For the determination of K_a only protons **a**, **b**, **c**, and **d** of **5** were monitored, because proton **e** shifted into a spectral region with overlapping signals of **4** and could not be traced unambiguously. The NMR data were analyzed with the *Bindfit* tool provided on *supramolecular.org*²⁻³ assuming a 1:1 stoichiometry. A binding constant $K_a = 1160 \text{ L} \cdot \text{mol}^{-1}$ was obtained from the best fit, while different assumed stoichiometries delivered significantly larger errors. This translates into a free energy change $\Delta G = -4.1 \text{ kcal} \cdot \text{mol}^{-1}$ upon binding.

A second independent titration was conducted to obtain an estimation for the errors occurring during quantitative assessment of the binding. This experiment gave a binding constant $K_a = 1020 \text{ L} \cdot \text{mol}^{-1}$, which translates into a free energy change $\Delta G = -4.0 \text{ kcal} \cdot \text{mol}^{-1}$.

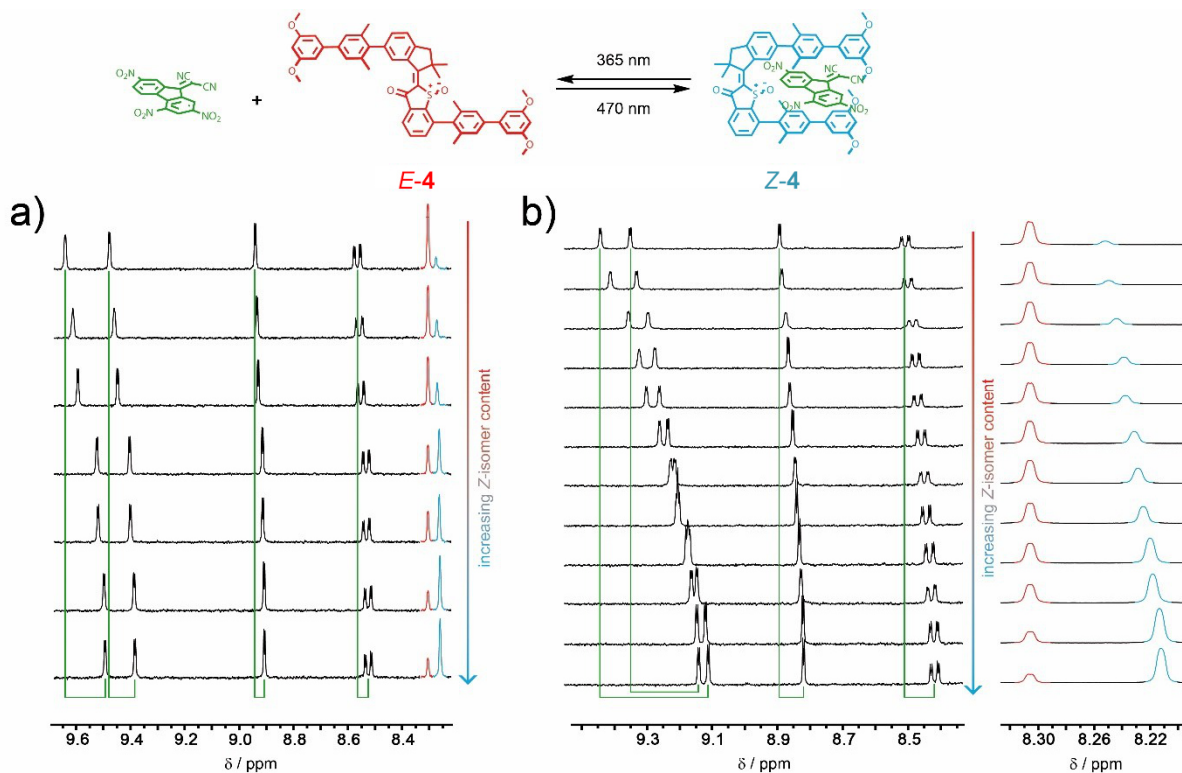


Figure S6: Determination of the binding constant K_a for formation of the association complex **Z-4** by NMR titration with the aid of light. Aromatic section of the ¹H-NMR spectra (400 MHz, 293 K, CDCl₃) recorded during the titration. The concentration of **5** was kept constant. a) ¹H-NMR spectra of *solution 1* with varying *E/Z* isomer ratio of **4** resulting in varying ratios between **5** and binding **Z-4**. b) ¹H-NMR spectra of *solution 2* with varying *E/Z* isomer ratio of **4** resulting in varying ratios between **5** and binding **Z-4**.

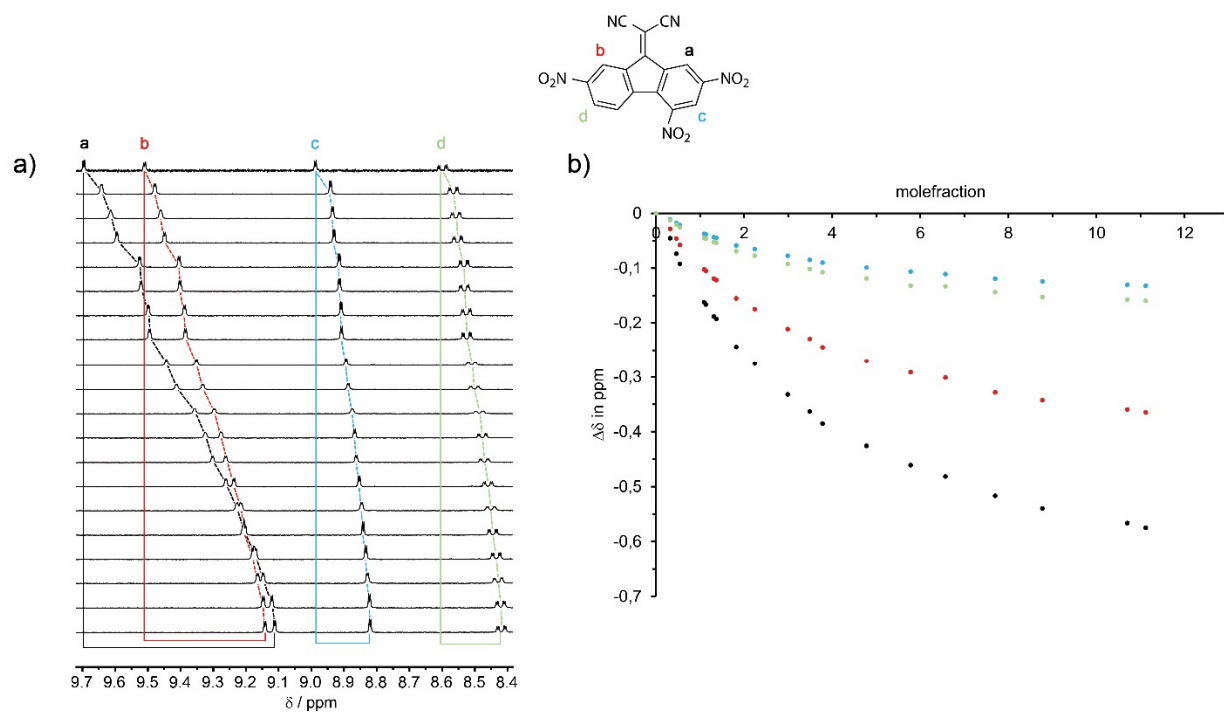


Figure S7: First NMR assessment of the supramolecular binding between Z-4 and **5**. a) Aromatic section of the ¹H-NMR spectra (400 MHz, 293 K, CDCl₃) recorded during the titration experiment. The concentration of **5** was kept constant and an increasing concentration of Z-4 is obtained by continuous photoirradiation with 470 nm light (from top to bottom). Shifts of indicative protons of **5** are labeled in color. b) Plot of the ratio **5**:Z-4 (mole fraction) against the corresponding shifts ($\Delta\delta = \delta_x - \delta_0$).

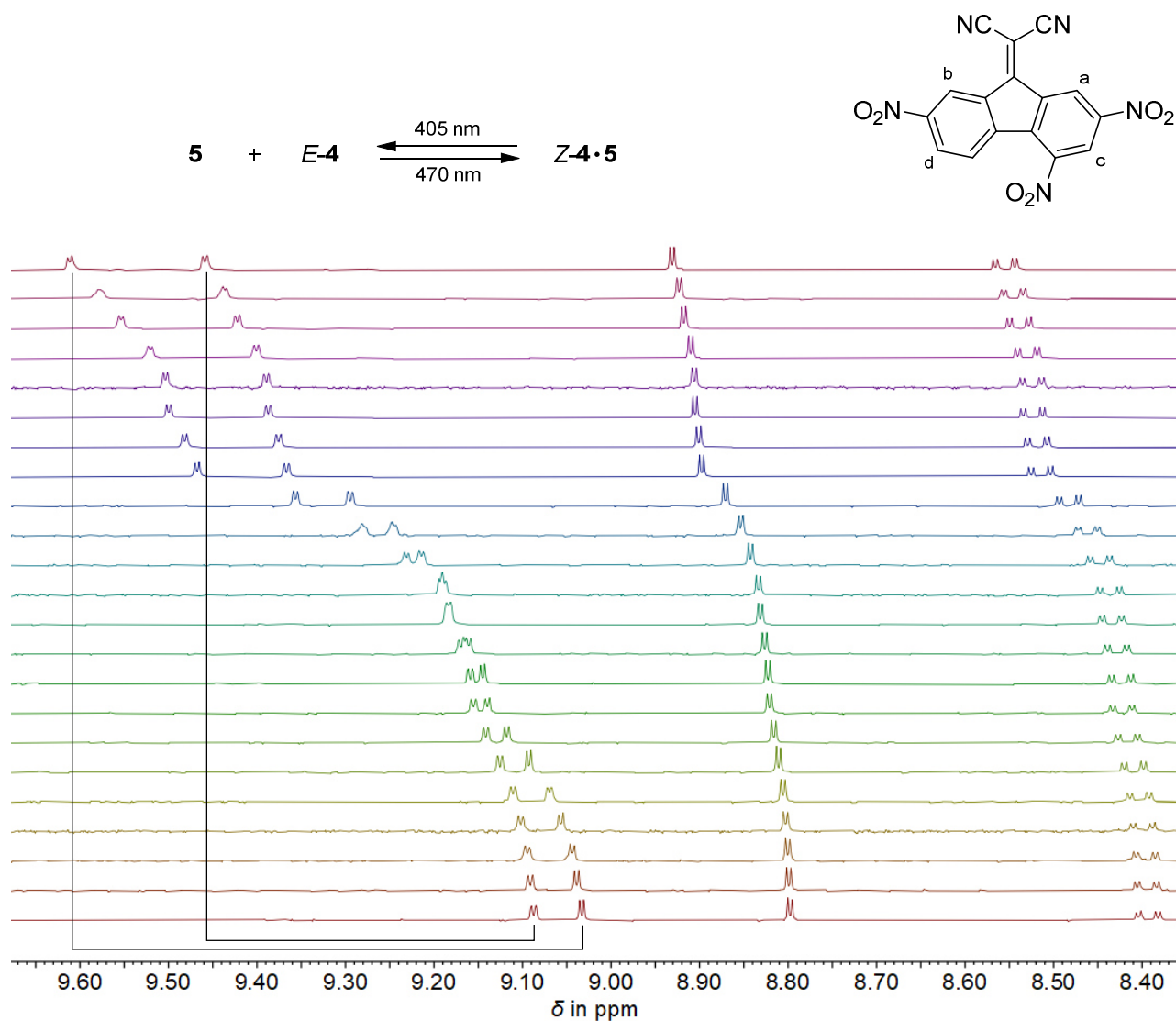


Figure S8: Second ^1H -NMR assessment of the supramolecular binding between **Z-4** and **5**. Aromatic section of the ^1H -NMR spectra (400 MHz, 293 K, CDCl_3) recorded during the titration experiment. The concentration of **5** was kept constant and an increasing concentration of **Z-4** is obtained by continuous photoirradiation with 470 nm light (from top to bottom).

Table S3: Chemical shifts of indicative protons of **5** observed in the $^1\text{H-NMR}$ spectra (400 MHz, 293 K, CDCl_3) during the first titration experiments. The concentration of **5** was kept constant while the concentration of **Z-4** was varied by irradiation with light of 365 nm or 470 nm wavelengths.

[5] in mol · L ⁻¹	[Z-4] in mol · L ⁻¹	δH_a	δH_b	δH_c	δH_d
2.75E-04	0.00E+00	9.6872	9.5067	8.9523	8.5783
2.75E-04	8.81E-05	9.6418	9.4785	8.9415	8.5656
2.75E-04	1.27E-04	9.6136	9.4609	8.9349	8.5578
2.75E-04	1.49E-04	9.5951	9.4490	8.9308	8.5527
2.75E-04	3.00E-04	9.5251	9.4044	8.9148	8.5333
2.75E-04	3.11E-04	9.5209	9.4017	8.9139	8.5321
2.75E-04	3.61E-04	9.4989	9.3877	8.9088	8.5259
2.75E-04	3.77E-04	9.4946	9.3851	8.9078	8.5248
2.75E-04	5.01E-04	9.4431	9.3516	8.8938	8.5094
2.75E-04	6.17E-04	9.4122	9.3319	8.8871	8.5011
2.75E-04	8.23E-04	9.3552	9.2955	8.8748	8.4862
2.75E-04	9.61E-04	9.3240	9.2773	8.8673	8.4768
2.75E-04	1.04E-03	9.3020	9.2620	8.8626	8.4709
2.75E-04	1.32E-03	9.2615	9.2365	8.8535	8.4597
2.75E-04	1.59E-03	9.2263	9.2152	8.8461	8.4463
2.75E-04	1.81E-03	9.2056	9.2056	8.8416	8.4451
2.75E-04	2.12E-03	9.1706	9.1785	8.8332	8.4346
2.75E-04	2.41E-03	9.1476	9.1641	8.8283	8.4255
2.75E-04	2.95E-03	9.1209	9.1472	8.8222	8.4210
2.75E-04	3.06E-03	9.1123	9.1417	8.8204	8.4186

Table S4: Chemical shifts of indicative protons of **5** observed in the ¹H-NMR spectra (400 MHz, 293 K, CDCl₃) during the second titration experiments. The concentration of **5** was kept constant while the concentration of **Z-4** was varied by irradiation with light of 365 nm or 470 nm wavelengths.

[5] in mol · L ⁻¹	[Z-4] in mol · L ⁻¹	δH _a	δH _b	δH _c	δH _d
6.89E-04	0.00E+00	9.6920	9.5093	8.9693	8.5885
6.89E-04	2.48E-04	9.6118	9.4587	8.9310	8.5551
6.89E-04	3.28E-04	9.5784	9.4384	8.9231	8.5453
6.89E-04	3.99E-04	9.5535	9.4222	8.9178	8.5388
6.89E-04	5.06E-04	9.5206	9.4008	8.9101	8.5295
6.89E-04	5.32E-04	9.5034	9.3896	8.9058	8.5244
6.89E-04	5.86E-04	9.4997	9.3874	8.9051	8.5236
6.89E-04	6.39E-04	9.4817	9.3752	8.9010	8.5185
6.89E-04	7.10E-04	9.4677	9.3668	8.8976	8.5145
6.89E-04	1.19E-03	9.35645	9.2947	8.8707	8.4827
6.89E-04	1.59E-03	9.2817	9.2476	8.8529	8.4613
6.89E-04	2.02E-03	9.2311	9.2144	8.8423	8.4477
6.89E-04	2.42E-03	9.1949	9.1858	8.8334	8.4367
6.89E-04	2.58E-03	9.1857	9.1811	8.8314	8.4343
6.89E-04	2.93E-03	9.1608	9.1697	8.8265	8.4283
6.89E-04	3.21E-03	9.1450	9.1589	8.8228	8.4265
6.89E-04	3.41E-03	9.1397	9.1556	8.8211	8.4224
6.89E-04	4.02E-03	9.1180	9.1414	8.8161	8.4162
6.89E-04	4.95E-03	9.0929	9.1257	8.8108	8.4095
6.89E-04	5.78E-03	9.0697	9.1108	8.8057	8.4030
6.89E-04	6.40E-03	9.0565	9.1020	8.8028	8.3992
6.89E-04	7.22E-03	9.0438	9.0945	8.8004	8.3962
6.89E-04	7.64E-03	9.0388	9.0911	8.7992	8.3946
6.89E-04	8.26E-03	9.0330	9.0869	8.7979	8.3930

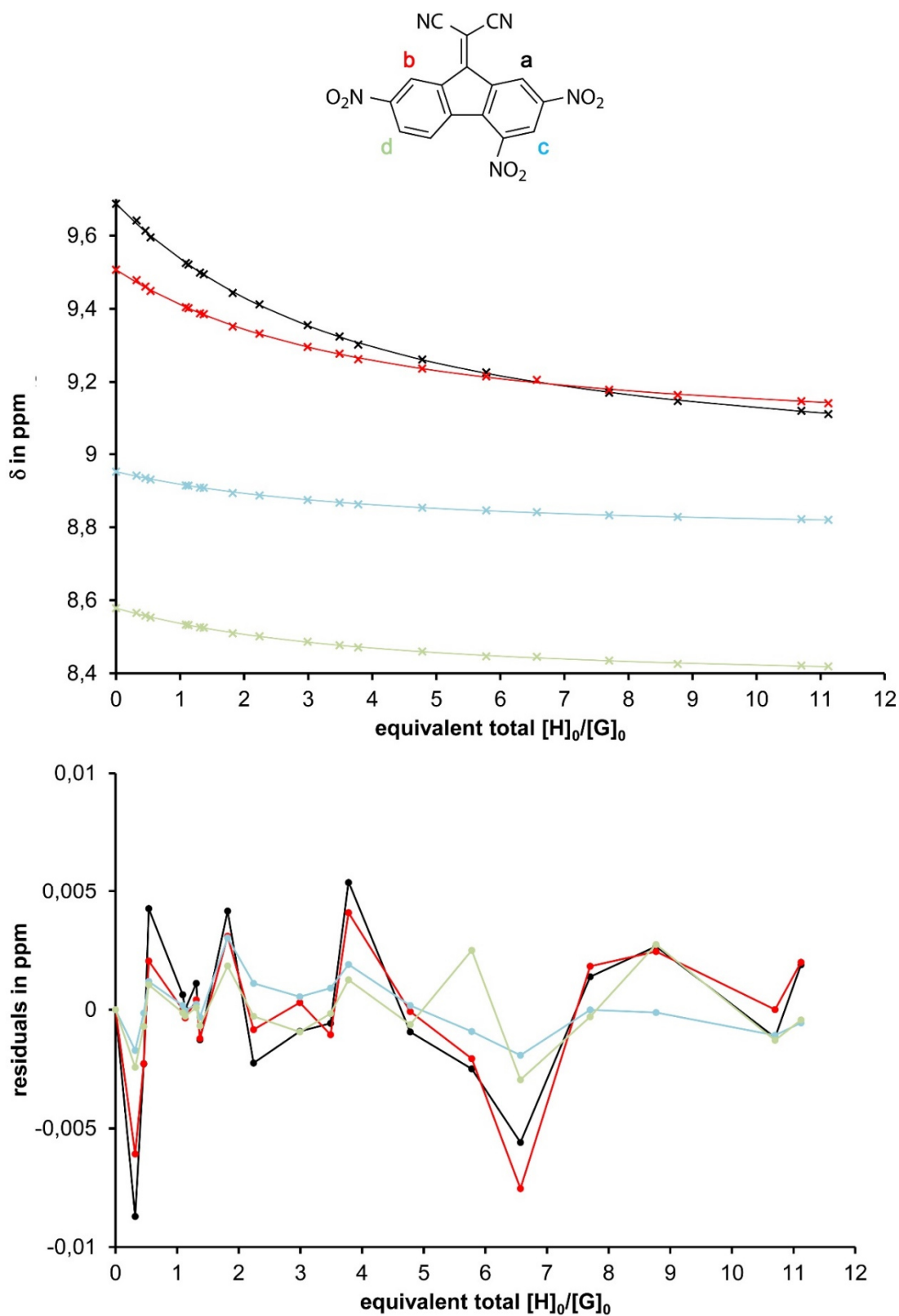


Figure S9: Assessment of the first titration data for the binding between Z-4 and 5. Top: plot of the chemical shift changes ($^1\text{H-NMR}$ (400 MHz, 293 K, CDCl_3)) of indicative protons of 5 occurring during the titration with Z-4 (crosses) and nonlinear regression fit (*Bindfit* tool, solid lines). Bottom: deviation of the measured $^1\text{H-NMR}$ shifts from the fit.

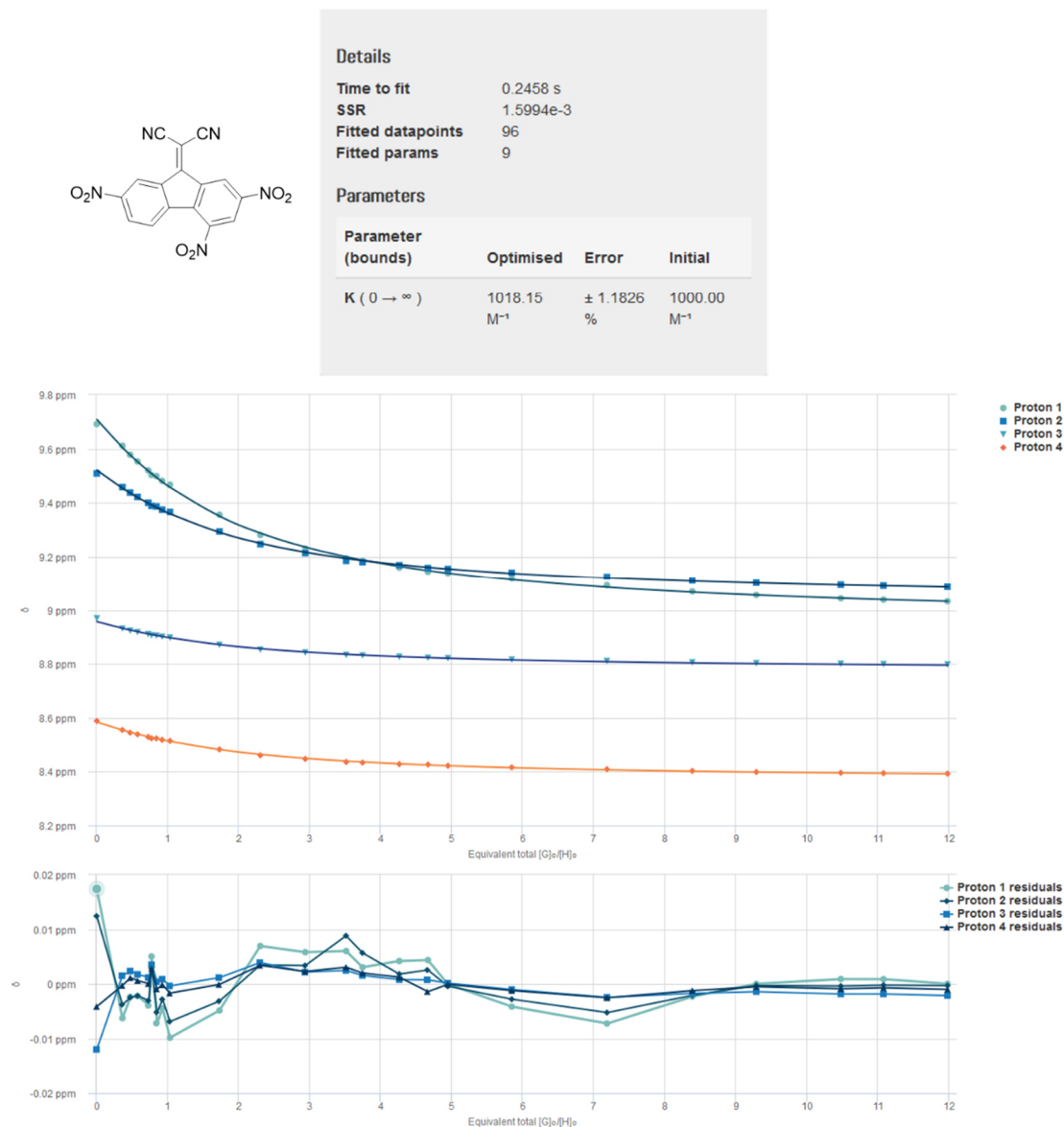


Figure S10: Assessment of the second titration data for the binding between **Z-4** and **5**. Top: plot of the chemical shift changes (¹H-NMR (400 MHz, 293 K, CDCl₃)) of indicative protons of **5** occurring during the titration with **Z-4** (crosses) and nonlinear regression fit (*Bindfit* tool, solid lines). Bottom: deviation of the measured ¹H-NMR shifts from the fit.

Van't Hoff analysis

A van't Hoff analysis was conducted in order to determine the contributions of ΔH and ΔS to the binding between **Z-4** and **5**. Two further titrations at different temperatures (253K and 273K) were carried out. For the titrations at different temperatures two samples were prepared similarly to the method described above (Stock solution of **5**: 0.433 mg in 4 ml CDCl₃; *solution 1*: 0.717 mg of **4** in 1.5 mL of the stock solution; *solution 2*: 5.533 mg of **4** in 1.5 mL of the

stock solution). The binding constants were obtained from fitting the corresponding titration data with *Bindfit* giving $K_a = 4136 \text{ L} \cdot \text{mol}^{-1}$ at 253 K and $K_a = 1833 \text{ L} \cdot \text{mol}^{-1}$ at 273 K.

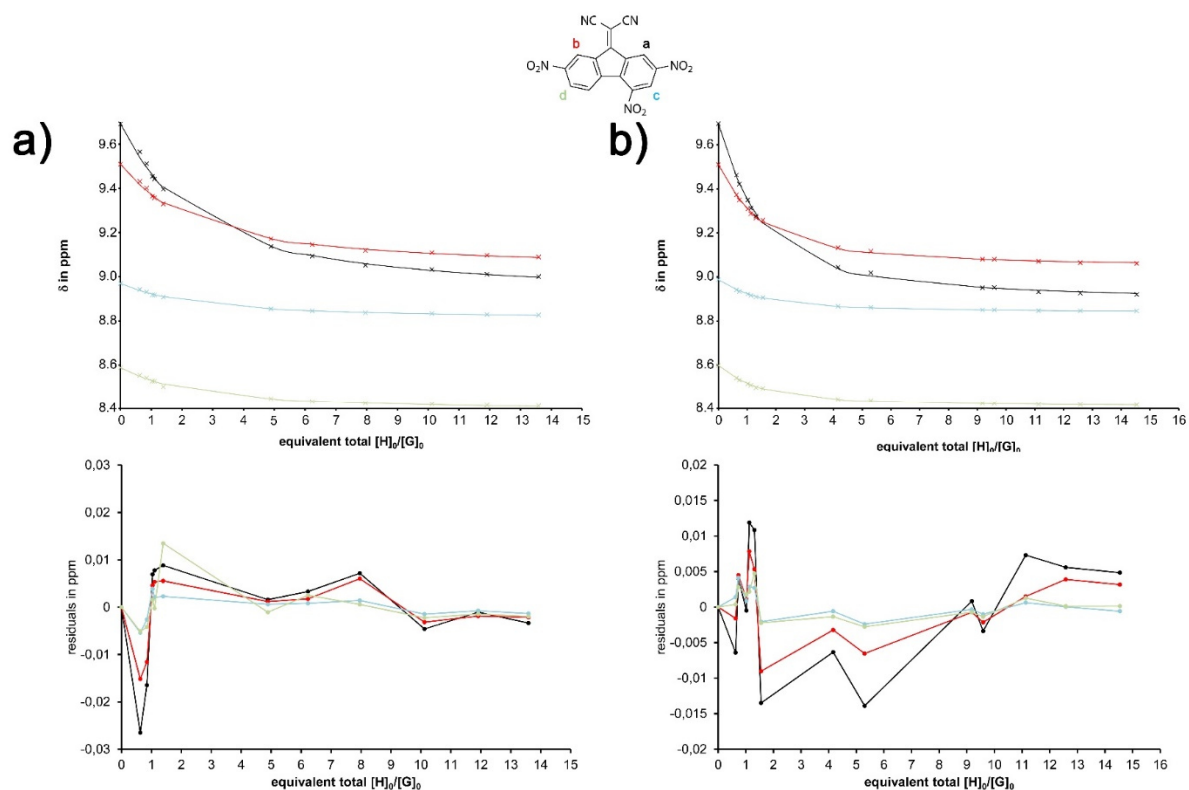


Figure S11: Quantitative assessment of supramolecular binding between Z-4 and 5 at different temperatures. a) Top: plot of the chemical shift changes ($^1\text{H-NMR}$ (400 MHz, 273 K, CDCl_3)) of indicative protons of 5 occurring during the titration with Z-4 (crosses) and nonlinear regression fit (*Bindfit* tool, solid lines). Bottom: deviation of the measured $^1\text{H-NMR}$ shifts from the fit. b) Top: plot of the shift of indicative protons of 5 ($^1\text{H-NMR}$ (400 MHz, 253 K, CDCl_3)) during the titration (crosses) and nonlinear regression fit (*Bindfit* tool, solid lines). Bottom: deviation of the measured $^1\text{H-NMR}$ shifts from the fit.

Table S5: Chemical shifts of indicative protons of **5** observed in the ¹H-NMR spectra (400 MHz, 273 K, CDCl₃) during the titration experiments. The concentration of **5** was kept constant while the concentration of Z-4 was varied by irradiation with light of 365 nm or 470 nm wavelengths.

[5] in mol · L ⁻¹	[Z-4] in mol · L ⁻¹	δH _a	δH _b	δH _c	δH _d
2.98E-04	0.00E+00	9.692	9.5093	8.9693	8.5885
2.98E-04	1.88E-04	9.5653	9.4313	8.943	8.5543
2.98E-04	2.53E-04	9.5117	9.4012	8.9312	8.5422
2.98E-04	3.10E-04	9.4542	9.3643	8.9177	8.5277
2.98E-04	3.29E-04	9.4424	9.3569	8.9172	8.5267
2.98E-04	4.16E-04	9.3963	9.3293	8.9077	8.5014
2.98E-04	1.46E-03	9.1372	9.1717	8.8543	8.4476
2.98E-04	1.86E-03	9.093	9.1453	8.8453	8.4331
2.98E-04	2.37E-03	9.0519	9.1184	8.837	8.4255
2.98E-04	3.02E-03	9.0328	9.1088	8.8335	8.4204
2.98E-04	3.55E-03	9.0113	9.0966	8.8291	8.415
2.98E-04	4.05E-03	9.0007	9.089	8.827	8.4122

Table S6: Chemical shifts of indicative protons of **5** observed in the ¹H-NMR spectra (400 MHz, 253 K, CDCl₃) during the titration experiments. The concentration of **5** was kept constant while the concentration of Z-4 was varied by irradiation with light of 365 nm or 470 nm wavelengths.

[5] in mol · L ⁻¹	[Z-4] in mol · L ⁻¹	δH _a	δH _b	δH _c	δH _d
2.98E-04	0.00E+00	9.696	9.5102	8.988	8.599
2.98E-04	1.88E-04	9.4624	9.373	8.9422	8.5418
2.98E-04	2.18E-04	9.4218	9.3495	8.9339	8.5322
2.98E-04	3.04E-04	9.3499	9.3086	8.923	8.5152
2.98E-04	3.37E-04	9.3124	9.2874	8.9164	8.5088
2.98E-04	3.90E-04	9.2764	9.2685	8.9097	8.4975
2.98E-04	4.62E-04	9.2583	9.2583	8.9066	8.4944
2.98E-04	1.24E-03	9.0445	9.133	8.8669	8.4446
2.98E-04	1.58E-03	9.019	9.1172	8.8626	8.4382
2.98E-04	2.74E-03	8.9517	9.081	8.8508	8.4237
2.98E-04	2.86E-03	8.9528	9.0806	8.8509	8.4236
2.98E-04	3.32E-03	8.9325	9.0714	8.8475	8.4187
2.98E-04	3.75E-03	8.9273	9.065	8.8468	8.4182
2.98E-04	4.33E-03	8.9209	9.0616	8.8461	8.4165

For the determination of ΔH and ΔS $\ln K_a$ was plotted against $\frac{1}{T}$.

$$\Delta G = -RT \ln K_a \quad (\text{eq. 3})$$

and

$$\Delta G = \Delta H - T\Delta S \quad (\text{eq. 4})$$

implies

$$\ln K_a = \frac{1}{T} \cdot -\frac{\Delta H}{R} + \frac{\Delta S}{R} \quad (\text{eq. 5})$$

Thus ΔS and ΔH can then be determined with:

$$\Delta S = \textit{intercept} \cdot R \quad (\text{eq. 6})$$

$$\Delta H = -\textit{slope} \cdot R \quad (\text{eq. 7})$$

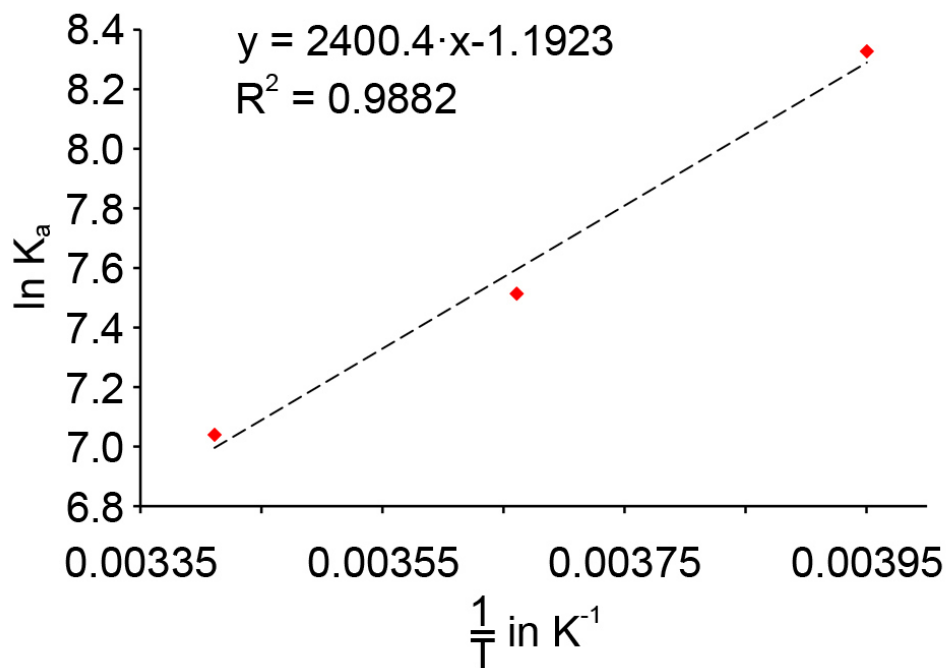


Figure S12: Van't Hoff plot of the natural logarithm of the binding constant K_a for association of Z-4 with **5** against $1/T$ (red squares). The dashed line represents the linear fit of the three points.

The resulting enthalpy and entropy contributions are:

$$\Delta H = -4.77 \text{ kcal/mol and } \Delta S = -2.37 \frac{\text{cal}}{\text{K}}.$$

Binding affinities between tweezers Z-3 and Z-4 and guest molecules 6 - 8

For titration experiments involving unoxidized tweezers **3** and guests **6 - 8** five solutions, altogether covering the range from 0.24–15.1 equiv. of Z-**3**, were prepared. Because of solubility issues titrations for guests **6** and **8** were conducted in CD₂Cl₂ solution. Therefore, 0.7 mL of a stock solution of the respective guest compound (1.00 mg in 4 mL CDCl₃ (**7**) or CD₂Cl₂ (**6** and **8**) for individual concentrations see Tables S7, S8, S11, S12, S15, and S16) was added to 0.66 equiv. (range: 0.24–0.55 equiv. Z-**3**), 1.50 equiv. (range: 0.55–1.26 equiv. Z-**3**), 3.50 equiv. (range: 1.30–2.94 equiv. Z-**3**), 8.00 equiv. (range: 2.96–6.72 equiv. Z-**3**), and 18.0 equiv. (range: 6.66–15.1 equiv. Z-**3**) of solid tweezers **3** respectively. With each solution a titration experiment using the photoirradiation method described above was conducted and four to five measurement points were recorded.

For titration experiments involving oxidized tweezers **4** and guests **6 - 8** three solutions, altogether covering the range from 0.20–13.0 equiv. of Z-**4** were prepared. Because of solubility issues titrations for guests **6** and **8** were conducted in CD₂Cl₂ solution. Therefore, 0.7 mL of a stock solution of the guest compound (1.00 mg in 4 mL CDCl₃ (**7**) or CD₂Cl₂ (**6** and **8**), for individual concentrations see Tables S9, S10, S13, S14, S17, and S18) was added to 1.18 equiv. (range: 0.20–0.97 equiv. Z-**4**), 5.76 equiv. (range: 0.98–4.78 equiv. Z-**4**) and 15.0 equiv. (range: 2.55–13.0 equiv. Z-**4**) of solid tweezers **4** respectively. With each solution a titration experiment using the photoirradiation method described above was conducted and seven to eight measurement points were recorded.

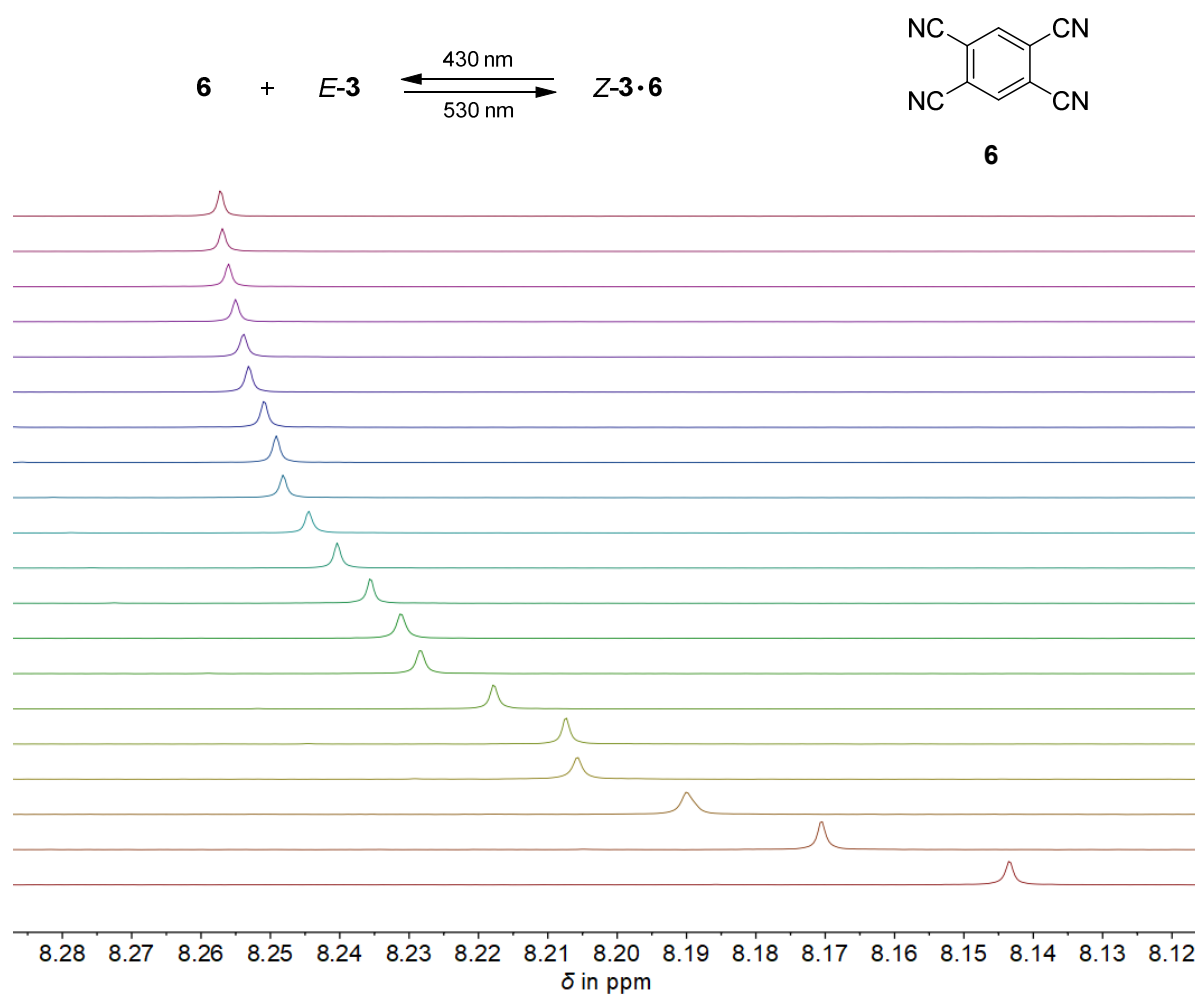


Figure S13: Determination of the binding constant K_a for formation of the association complex $Z\text{-}\mathbf{3}\cdot\mathbf{6}$ by NMR titration with the aid of light. One out of two independent experiments is shown exemplarily. Aromatic section of the ^1H -NMR spectra (400 MHz, 293 K, CD_2Cl_2) recorded during the titration showing the shift of indicative proton H_1 . The concentration of **6** was kept constant. Irradiation leads to varying E/Z isomer ratio of **3** resulting in varying ratios between **6** and binding $Z\text{-}\mathbf{3}$ (top highest $E\text{-}\mathbf{3}$ isomer content, bottom highest $Z\text{-}\mathbf{3}$ isomer content).

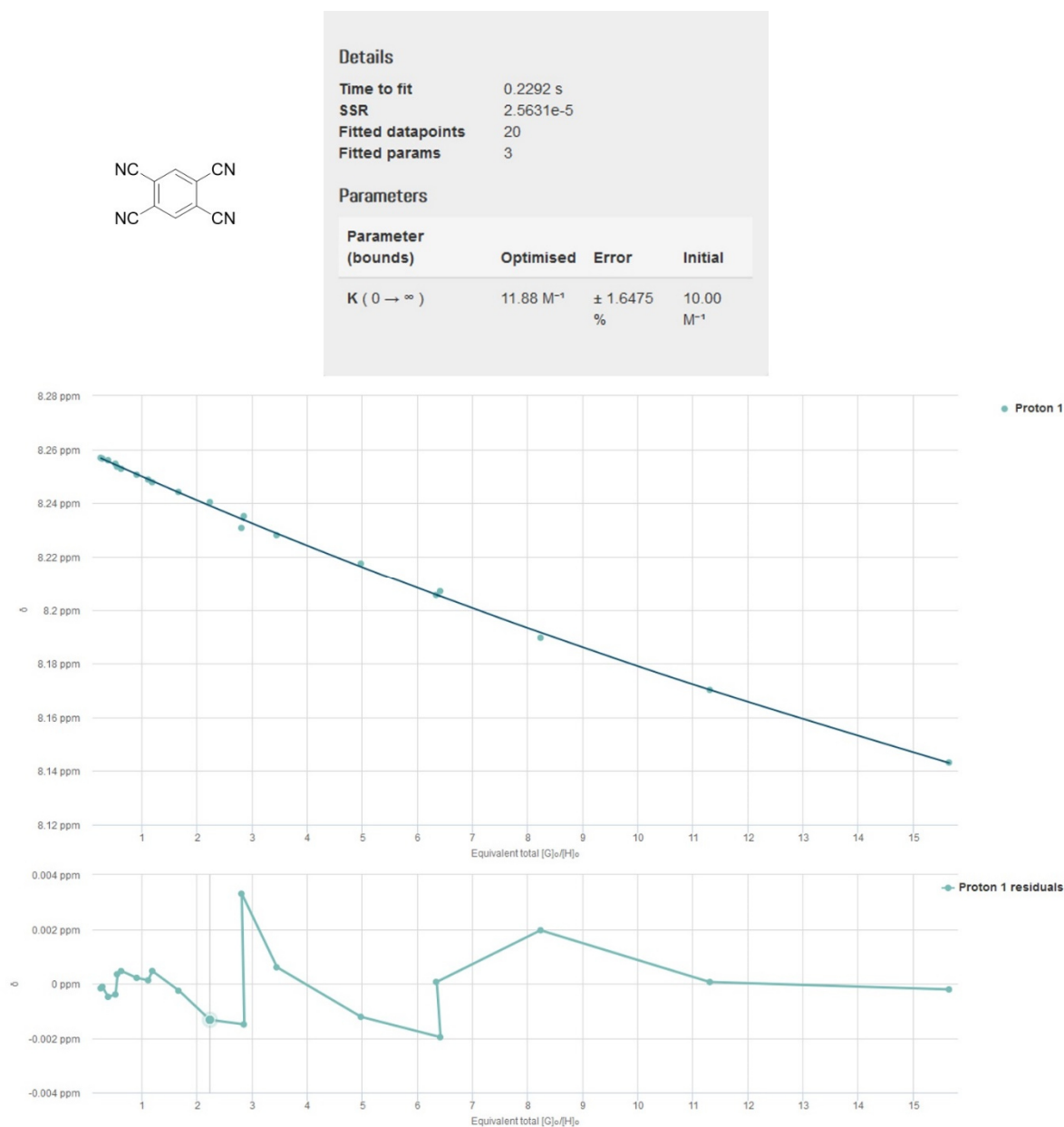


Figure S14: Assessment of the first measured titration data for the binding between **Z-3** and **6**. Top: plot of the chemical shift changes (¹H-NMR (400 MHz, 293 K, CD₂Cl₂)) of indicative proton H₁ of **6** occurring during the titration with **Z-3** (dots) and nonlinear regression fit (*Bindfit* tool, solid lines). Bottom: deviation of the measured ¹H-NMR shifts from the fit.

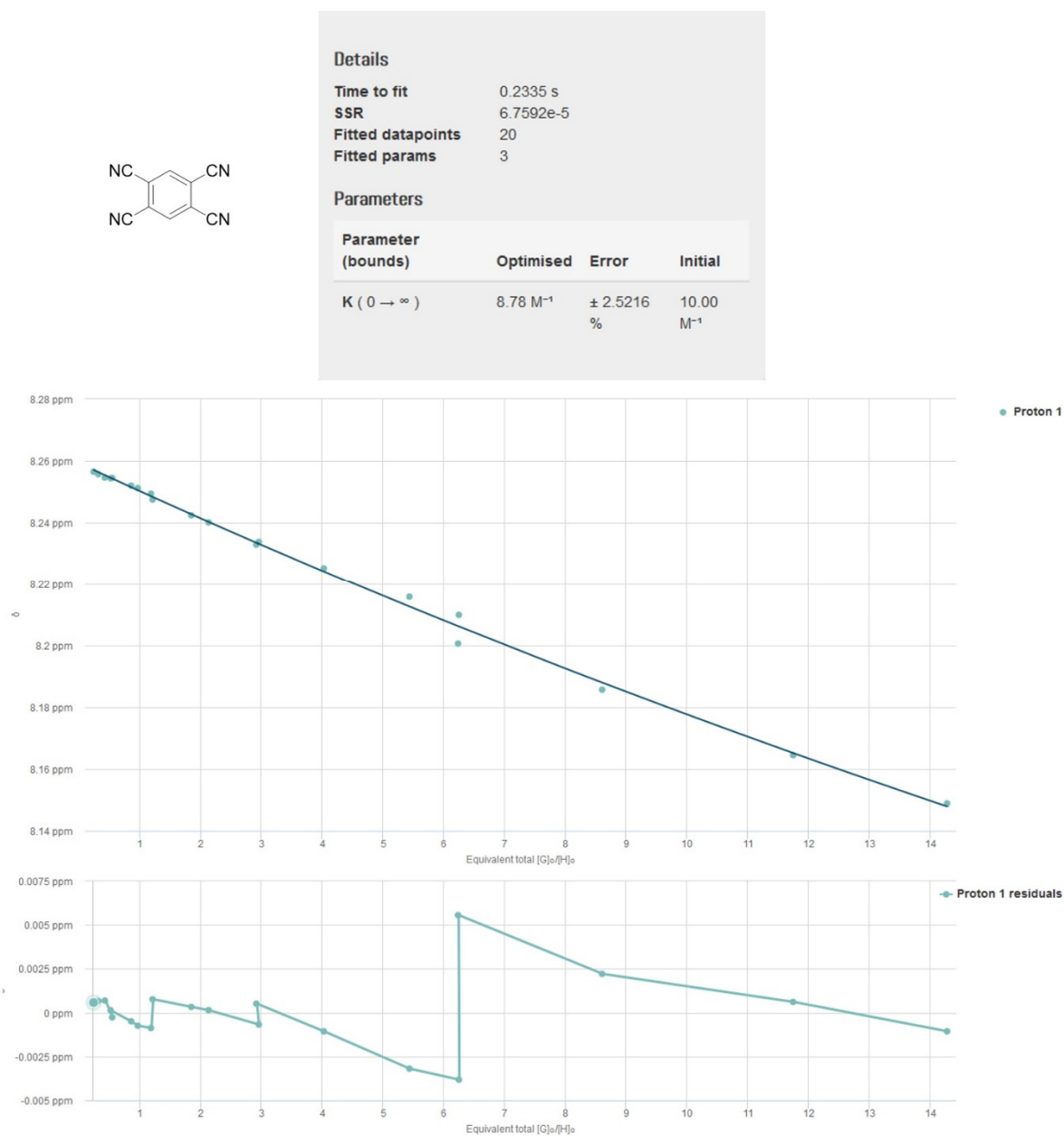


Figure S15: Assessment of the second measured titration data for the binding between **Z-3** and **6**. Top: plot of the chemical shift changes (¹H-NMR (400 MHz, 293 K, CD₂Cl₂)) of indicative proton H₁ of **6** occurring during the titration with **Z-3** (dots) and nonlinear regression fit (*Bindfit* tool, solid lines). Bottom: deviation of the measured ¹H-NMR shifts from the fit.

Table S7: Chemical shifts of indicative proton H₁ of **6** observed in the ¹H-NMR spectra (400 MHz, 293 K, CD₂Cl₂) during the first titration experiment. The concentration of **6** was kept constant while the concentration of Z-**3** was varied by irradiation with light of 430 nm or 530 nm wavelengths.

[6] in mol · L ⁻¹	[Z- 3] in mol · L ⁻¹	δH ₁
1.40E-03	3.52E-04	8.2569
1.40E-03	3.89E-04	8.2566
1.40E-03	5.37E-04	8.2560
1.40E-03	7.22E-04	8.2547
1.40E-03	7.77E-04	8.2536
1.40E-03	8.82E-04	8.2528
1.40E-03	1.26E-03	8.2506
1.40E-03	1.55E-03	8.2488
1.40E-03	1.66E-03	8.2478
1.40E-03	2.34E-03	8.2442
1.40E-03	3.12E-03	8.2404
1.40E-03	4.00E-03	8.2352
1.40E-03	3.93E-03	8.2308
1.40E-03	4.83E-03	8.2281
1.40E-03	6.96E-03	8.2175
1.40E-03	8.98E-03	8.2070
1.40E-03	8.89E-03	8.2055
1.40E-03	1.15E-02	8.1896
1.40E-03	1.58E-02	8.1702
1.40E-03	2.19E-02	8.1432

Table S8: Chemical shifts of indicative proton H₁ of **6** observed in the ¹H-NMR spectra (400 MHz, 293 K, CD₂Cl₂) during the second titration experiment. The concentration of **6** was kept constant while the concentration of **Z-3** was varied by irradiation with light of 430 nm or 530 nm wavelengths.

[6] in mol · L ⁻¹	[Z-3] in mol · L ⁻¹	δH ₁
1.40E-03	3.32E-04	8.2565
1.40E-03	4.42E-04	8.2557
1.40E-03	6.07E-04	8.2546
1.40E-03	7.72E-04	8.2545
1.40E-03	7.25E-04	8.2544
1.40E-03	1.20E-03	8.2520
1.40E-03	1.36E-03	8.2512
1.40E-03	1.67E-03	8.2494
1.40E-03	1.71E-03	8.2475
1.40E-03	2.59E-03	8.2424
1.40E-03	2.99E-03	8.2401
1.40E-03	4.14E-03	8.2338
1.40E-03	4.10E-03	8.2329
1.40E-03	5.64E-03	8.2252
1.40E-03	7.61E-03	8.2158
1.40E-03	8.76E-03	8.2099
1.40E-03	8.74E-03	8.2006
1.40E-03	1.21E-02	8.1857
1.40E-03	1.65E-02	8.1645
1.40E-03	2.00E-02	8.1489

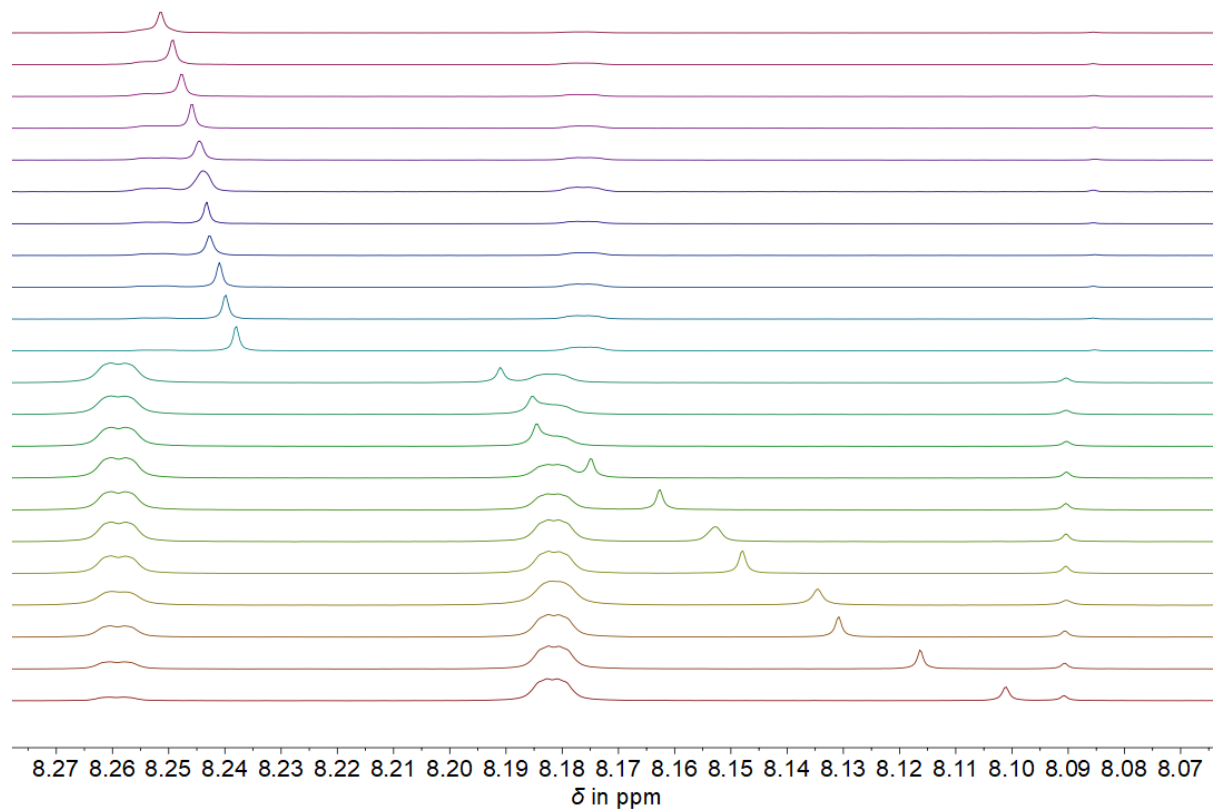
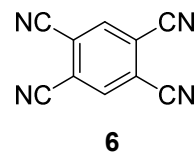
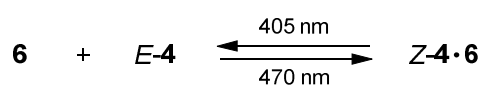
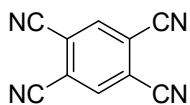


Figure S16: Determination of the binding constant K_a for formation of the association complex $Z\text{-}\mathbf{4}\cdot\mathbf{6}$ by NMR titration with the aid of light. One out of two independent experiments is shown exemplarily. Aromatic section of the $^1\text{H-NMR}$ spectra (400 MHz, 293 K, CD_2Cl_2) recorded during the titration showing the shift of indicative proton H_1 . The concentration of **6** was kept constant. Irradiation leads to varying E/Z isomer ratio of **4** resulting in varying ratios between **6** and binding $Z\text{-}\mathbf{4}$ (top highest $E\text{-}\mathbf{4}$ isomer content, bottom highest $Z\text{-}\mathbf{4}$ isomer content).



Details

Time to fit 0.2473 s
SSR 7.6717e-6
Fitted datapoints 22
Fitted params 3

Parameters

Parameter (bounds)	Optimised	Error	Initial
K (0 → ∞)	26.12 M ⁻¹	± 0.4868 %	20.00 M ⁻¹

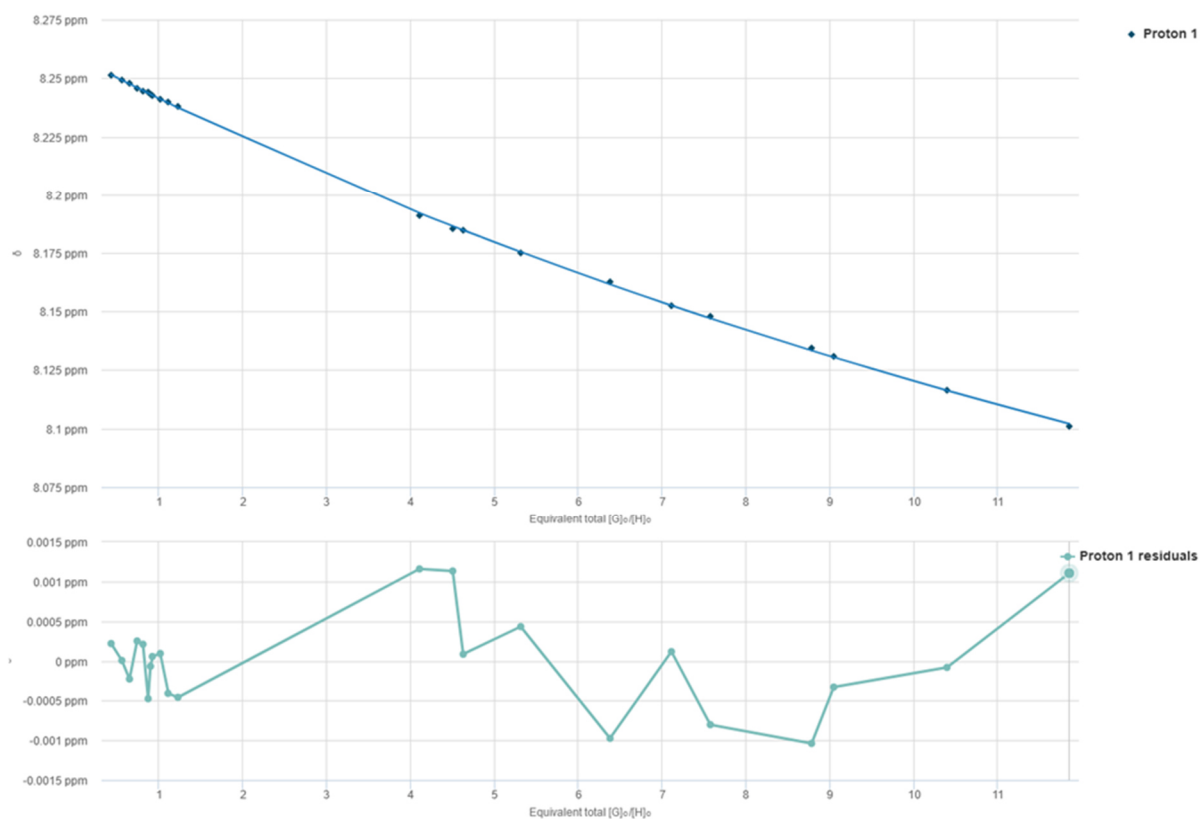
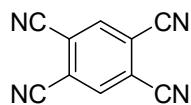


Figure S17: Assessment of the first measured titration data for the binding between Z-4 and 6. Top: plot of the chemical shift changes (¹H-NMR (400 MHz, 293 K, CD₂Cl₂)) of indicative proton H₁ of 6 occurring during the titration with Z-4 (dots) and nonlinear regression fit (*Bindfit* tool, solid lines). Bottom: deviation of the measured ¹H-NMR shifts from the fit.



Details

Time to fit 0.3639 s
SSR 1.7291e-5
Fitted datapoints 20
Fitted params 3

Parameters

Parameter (bounds)	Optimised	Error	Initial
K (0 → ∞)	24.85 M ⁻¹	± 0.7700 %	20.00 M ⁻¹

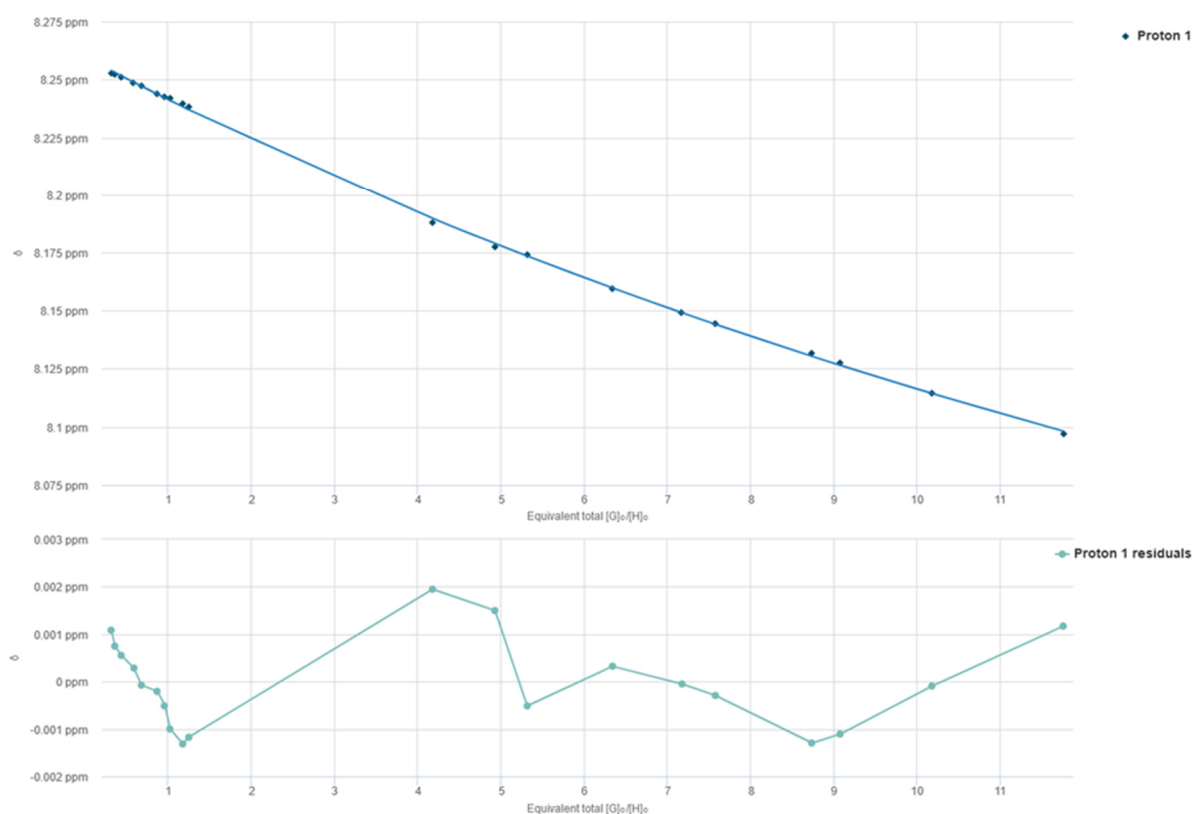


Figure S18: Assessment of the second measured titration data for the binding between **Z-4** and **6**. Top: plot of the chemical shift changes (¹H-NMR (400 MHz, 293 K, CD₂Cl₂)) of indicative proton H₁ of **6** occurring during the titration with **Z-4** (dots) and nonlinear regression fit (*Bindfit* tool, solid lines). Bottom: deviation of the measured ¹H-NMR shifts from the fit.

Table S9: Chemical shifts of indicative proton H₁ of **6** observed in the ¹H-NMR spectra (400 MHz, 293 K, CD₂Cl₂) during the first titration experiment. The concentration of **6** was kept constant while the concentration of Z-**4** was varied by irradiation with light of 405 nm or 470 nm wavelengths.

[6] in mol · L ⁻¹	[Z- 4] in mol · L ⁻¹	δH ₁
1.40E-03	6.00E-04	8.2513
1.40E-03	7.79E-04	8.2492
1.40E-03	9.07E-04	8.2478
1.40E-03	1.03E-03	8.2457
1.40E-03	1.13E-03	8.2445
1.40E-03	1.22E-03	8.2441
1.40E-03	1.26E-03	8.2432
1.40E-03	1.30E-03	8.2426
1.40E-03	1.42E-03	8.2410
1.40E-03	1.56E-03	8.2398
1.40E-03	1.72E-03	8.2379
1.40E-03	5.75E-03	8.1910
1.40E-03	6.30E-03	8.1854
1.40E-03	6.48E-03	8.1847
1.40E-03	7.44E-03	8.1750
1.40E-03	8.93E-03	8.1626
1.40E-03	9.95E-03	8.1525
1.40E-03	1.06E-02	8.1479
1.40E-03	1.23E-02	8.1344
1.40E-03	1.27E-02	8.1308
1.40E-03	1.46E-02	8.1164
1.40E-03	1.66E-02	8.1010

Table S10: Chemical shifts of indicative proton H₁ of **6** observed in the ¹H-NMR spectra (400 MHz, 293 K, CD₂Cl₂) during the first titration experiment. The concentration of **6** was kept constant while the concentration of Z-4 was varied by irradiation with light of 405 nm or 470 nm wavelengths.

[6] in mol · L ⁻¹	[Z-4] in mol · L ⁻¹	δH ₁
1.40E-03	4.41E-04	8.2528
1.40E-03	5.04E-04	8.2523
1.40E-03	6.09E-04	8.2511
1.40E-03	8.19E-04	8.2486
1.40E-03	9.46E-04	8.2473
1.40E-03	1.22E-03	8.2439
1.40E-03	1.34E-03	8.2426
1.40E-03	1.43E-03	8.2420
1.40E-03	1.64E-03	8.2396
1.40E-03	1.74E-03	8.2382
1.40E-03	5.84E-03	8.1879
1.40E-03	6.89E-03	8.1775
1.40E-03	7.44E-03	8.1741
1.40E-03	8.87E-03	8.1595
1.40E-03	1.00E-02	8.1492
1.40E-03	1.06E-02	8.1445
1.40E-03	1.22E-02	8.1317
1.40E-03	1.27E-02	8.1276
1.40E-03	1.43E-02	8.1145
1.40E-03	1.65E-02	8.0970

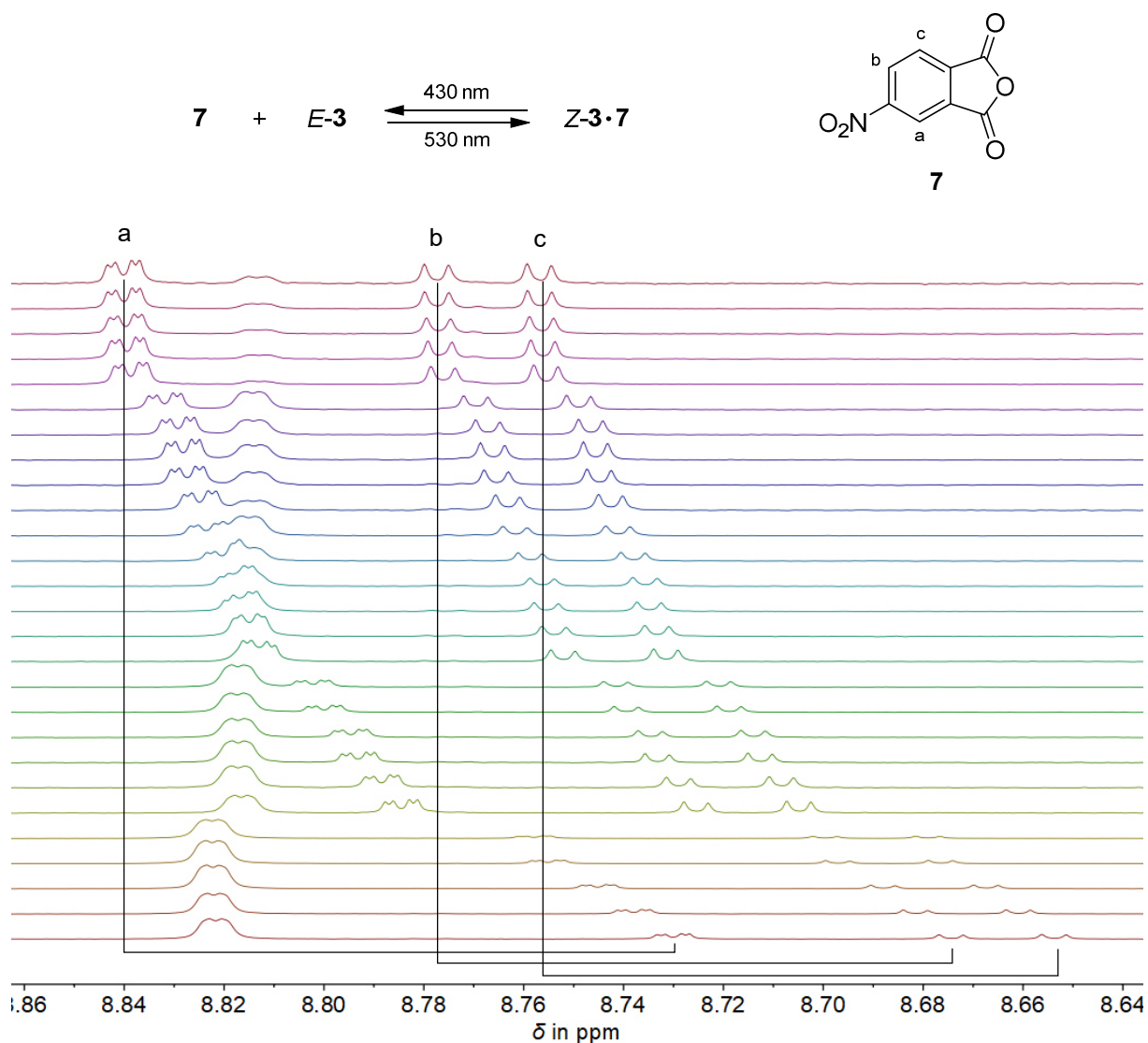


Figure S19: Determination of the binding constant K_a for formation of the association complex $Z-3 \cdot 7$ by NMR titration with the aid of light. One out of two independent experiments is shown exemplarily. Aromatic section of the $^1\text{H-NMR}$ spectra (400 MHz, 293 K, CDCl_3) recorded during the titration showing the shift of indicative protons H_a , H_b , and H_c of **7**. The concentration of **7** was kept constant. Irradiation leads to varying E/Z isomer ratio of **3** resulting in varying ratios between **7** and binding $Z-3$ (top highest $E-3$ isomer content, bottom highest $Z-3$ isomer content).

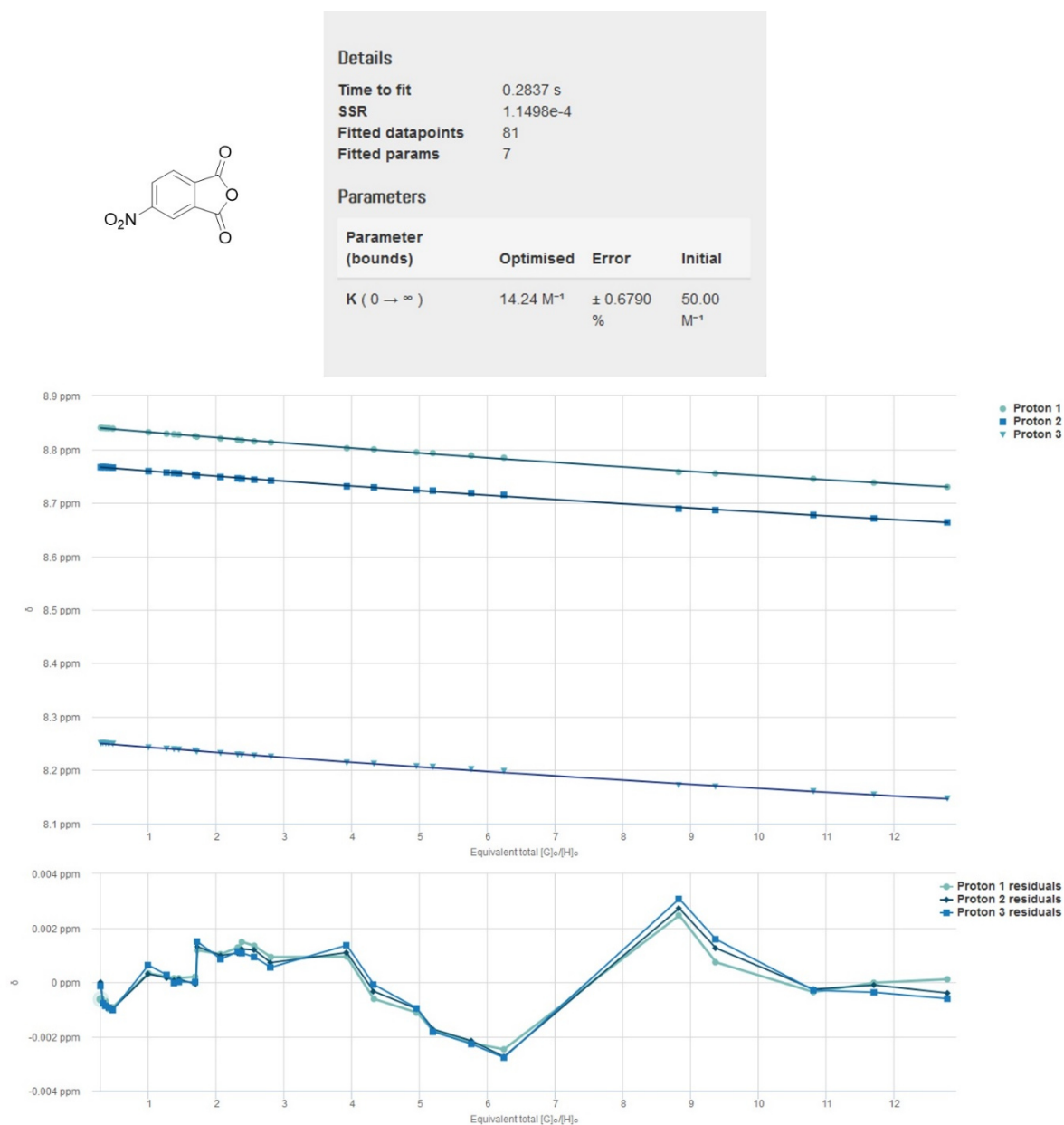
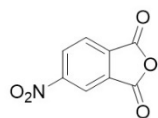


Figure S20: Assessment of the first measured titration data for the binding between Z-3 and 7. Top: plot of the chemical shift changes (¹H-NMR (400 MHz, 293 K, CDCl₃)) of indicative protons H_a, H_b, and H_c of 7 occurring during the titration with Z-3 (dots, squares, and triangles) and nonlinear regression fit (*Bindfit* tool, solid lines). Bottom: deviation of the measured ¹H-NMR shifts from the fit.



Details			
Time to fit	0.3548 s		
SSR	1.9460e-4		
Fitted datapoints	75		
Fitted params	7		
Parameters			
Parameter (bounds)	Optimised	Error	Initial
K (0 → ∞)	16.92 M ⁻¹	± 0.9209 %	50.00 M ⁻¹

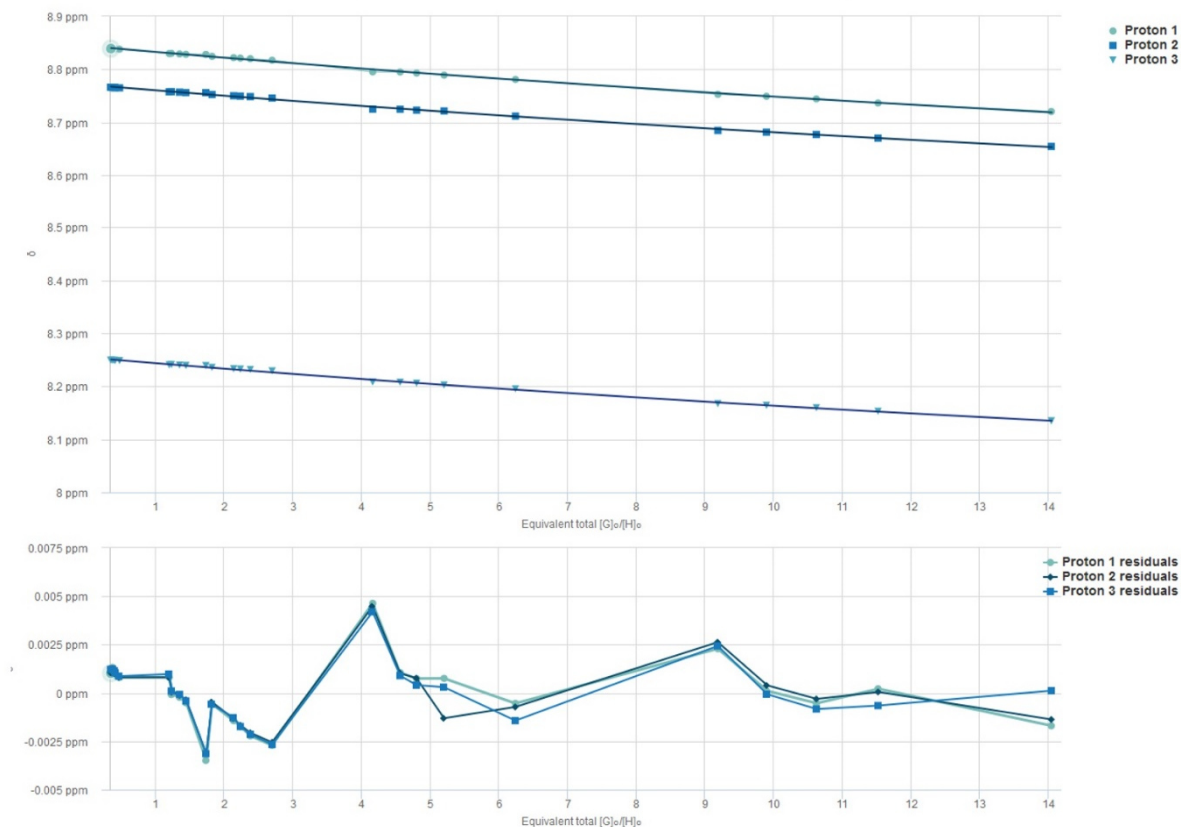


Figure S21: Assessment of the second measured titration data for the binding between Z-3 and 7. Top: plot of the chemical shift changes (¹H-NMR (400 MHz, 293 K, CDCl₃)) of indicative protons H_a, H_b, and H_c of 7 occurring during the titration with Z-3 (dots, squares, and triangles) and nonlinear regression fit (*Bindfit* tool, solid lines). Bottom: deviation of the measured ¹H-NMR shifts from the fit.

Table S11: Chemical shifts of indicative protons H_a, H_b, and H_c of **7** observed in the ¹H-NMR spectra (400 MHz, 293 K, CDCl₃) during the first titration experiment. The concentration of **7** was kept constant while the concentration of **Z-3** was varied by irradiation with light of 430 nm or 530 nm wavelengths.

[7] in mol · L ⁻¹	[Z-3] in mol · L ⁻¹	δH _a	δH _b	δH _c
1.29E-03	3.74E-04	8.8403	8.7667	8.2501
1.29E-03	4.17E-04	8.8400	8.7671	8.2504
1.29E-03	4.68E-04	8.8396	8.7668	8.2501
1.29E-03	5.27E-04	8.8394	8.7664	8.2497
1.29E-03	6.04E-04	8.8387	8.7659	8.2492
1.29E-03	1.28E-03	8.8319	8.7594	8.2423
1.29E-03	1.64E-03	8.8292	8.7569	8.2400
1.29E-03	1.78E-03	8.8281	8.7559	8.2392
1.29E-03	1.87E-03	8.8274	8.7552	8.2385
1.29E-03	2.19E-03	8.8248	8.7530	8.2361
1.29E-03	2.22E-03	8.8236	8.7514	8.2344
1.29E-03	2.67E-03	8.8202	8.7484	8.2317
1.29E-03	2.99E-03	8.8175	8.7460	8.2291
1.29E-03	3.08E-03	8.8166	8.7452	8.2285
1.29E-03	3.11E-03	8.8150	8.7436	8.2270
1.29E-03	3.62E-03	8.8130	8.7418	8.2251
1.29E-03	5.07E-03	8.8022	8.7313	8.2141
1.29E-03	5.59E-03	8.8000	8.7292	8.2120
1.29E-03	6.42E-03	8.7946	8.7243	8.2073
1.29E-03	6.73E-03	8.7931	8.7230	8.2061
1.29E-03	7.45E-03	8.7885	8.7187	8.2018
1.29E-03	8.07E-03	8.7845	8.7153	8.1983
1.29E-03	1.14E-02	8.7578	8.6894	8.1719
1.29E-03	1.21E-02	8.7552	8.6868	8.1693
1.29E-03	1.40E-02	8.7451	8.6778	8.1606
1.29E-03	1.51E-02	8.7380	8.6713	8.1543
1.29E-03	1.65E-02	8.7300	8.6642	8.1471

Table S12: Chemical shifts of indicative protons H_a, H_b, and H_c of **7** observed in the ¹H-NMR spectra (400 MHz, 293 K, CDCl₃) during the second titration experiment. The concentration of **7** was kept constant while the concentration of **Z-3** was varied by irradiation with light of 430 nm or 530 nm wavelengths.

[7] in mol · L ⁻¹	[Z-3] in mol · L ⁻¹	δH _a	δH _b	δH _c
1.29E-03	4.50E-04	8.8393	8.7664	8.2495
1.29E-03	4.85E-04	8.8387	8.7659	8.2492
1.29E-03	5.19E-04	8.8387	8.7658	8.2490
1.29E-03	5.44E-04	8.8386	8.7657	8.2489
1.29E-03	6.12E-04	8.8381	8.7653	8.2485
1.29E-03	1.55E-03	8.8300	8.7577	8.2407
1.29E-03	1.61E-03	8.8304	8.7580	8.2411
1.29E-03	1.75E-03	8.8293	8.7570	8.2401
1.29E-03	1.87E-03	8.8286	8.7563	8.2395
1.29E-03	2.25E-03	8.8284	8.7561	8.2392
1.29E-03	2.22E-03	8.8246	8.7526	8.2358
1.29E-03	2.35E-03	8.8221	8.7503	8.2333
1.29E-03	2.76E-03	8.8213	8.7496	8.2327
1.29E-03	2.89E-03	8.8203	8.7486	8.2317
1.29E-03	3.08E-03	8.8175	8.7460	8.2291
1.29E-03	3.49E-03	8.7954	8.7251	8.2082
1.29E-03	5.38E-03	8.7951	8.7249	8.2078
1.29E-03	5.90E-03	8.7931	8.7230	8.2061
1.29E-03	6.21E-03	8.7893	8.7215	8.2026
1.29E-03	6.73E-03	8.7810	8.7119	8.1952
1.29E-03	7.45E-03	8.7529	8.6848	8.1673
1.29E-03	8.07E-03	8.7493	8.6816	8.1643
1.29E-03	1.19E-02	8.7443	8.6770	8.1597
1.29E-03	1.28E-02	8.7367	8.6702	8.1530
1.29E-03	1.37E-02	8.7205	8.6546	8.1350

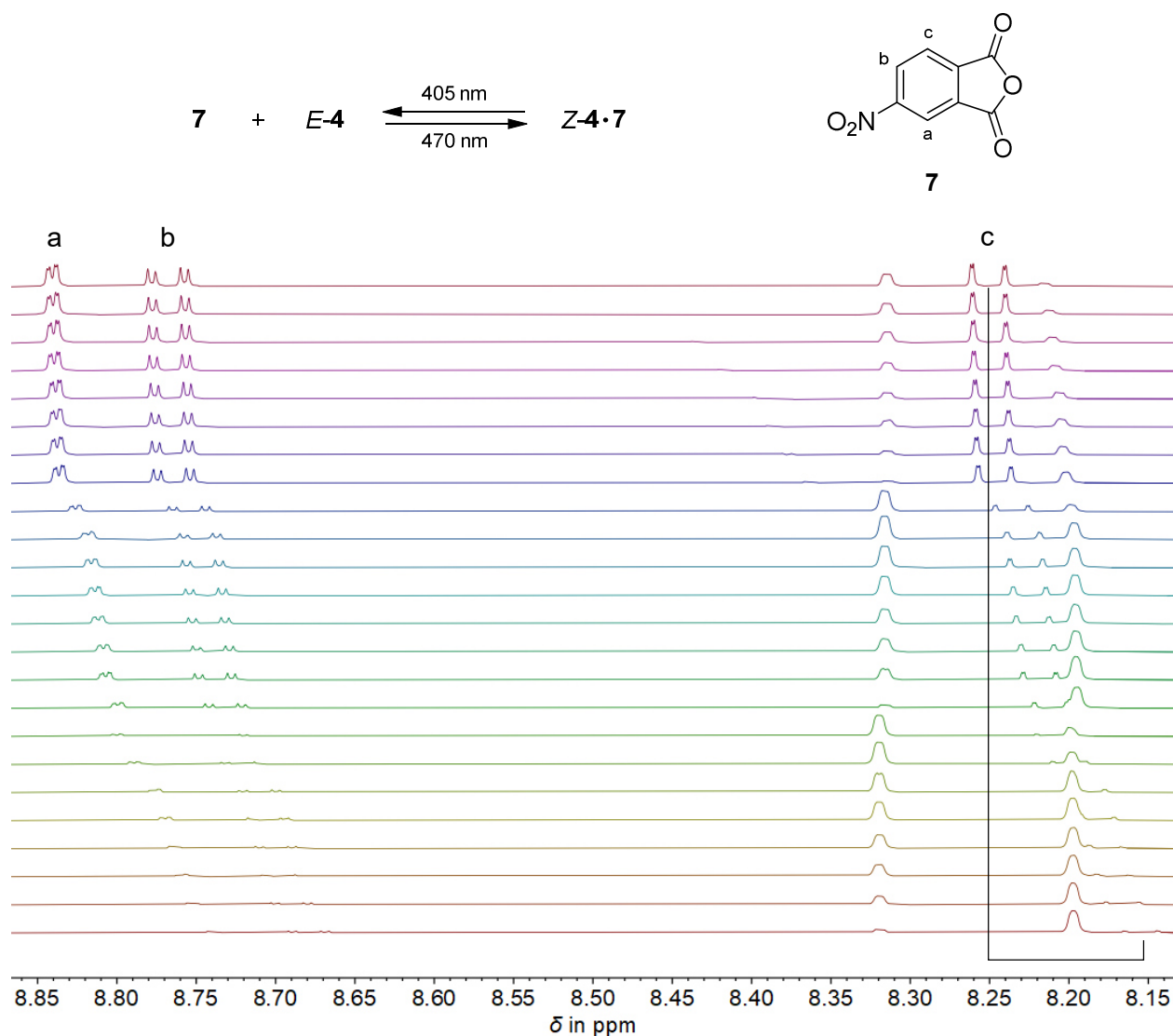


Figure S22: Determination of the binding constant K_a for formation of the association complex $Z-4 \cdot 7$ by NMR titration with the aid of light. One out of two independent experiments is shown exemplarily. Aromatic section of the ^1H -NMR spectra (400 MHz, 293 K, CDCl_3) recorded during the titration showing the shift of indicative protons H_a , H_b , and H_c of **7**. The concentration of **7** was kept constant. Irradiation leads to varying E/Z isomer ratio of **4** resulting in varying ratios between **7** and binding $Z-4$ (top highest $E-4$ isomer content, bottom highest $Z-4$ isomer content).

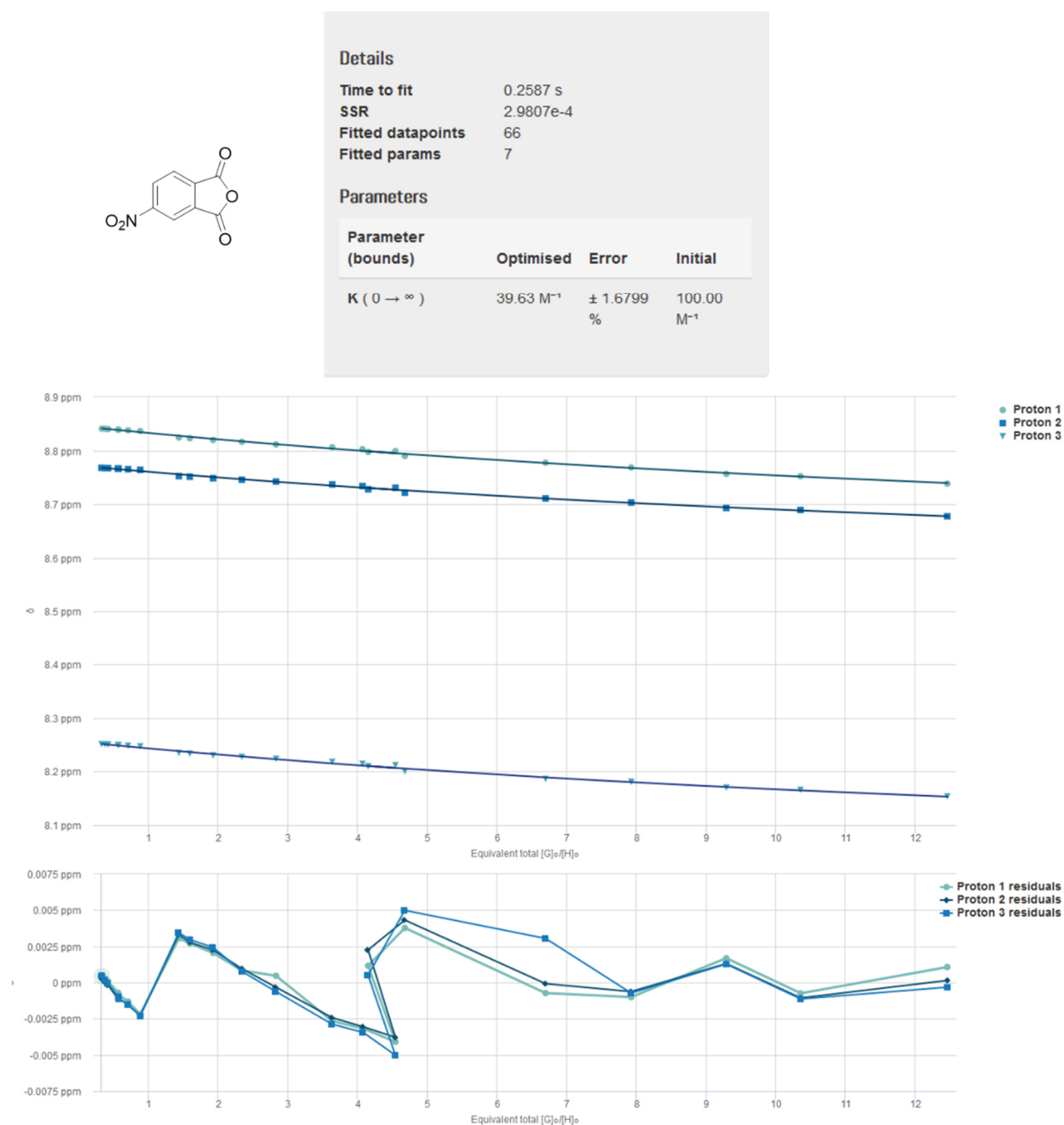
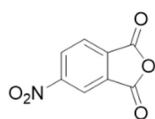


Figure S23: Assessment of the first measured titration data for the binding between Z-4 and 7. Top: plot of the chemical shift changes (¹H-NMR (400 MHz, 293 K, CD₂Cl₂)) of indicative protons H_a, H_b, and H_c of 7 occurring during the titration with Z-4 (dots, squares, and triangles) and nonlinear regression fit (*Bindfit* tool, solid lines). Bottom: deviation of the measured ¹H-NMR shifts from the fit.



Details

Time to fit 0.5710 s
 SSR 3.0196e-4
 Fitted datapoints 72
 Fitted params 7

Parameters

Parameter (bounds)	Optimised	Error	Initial
K (26 → 54)	30.21 M ⁻¹	± 1.4489 %	40.00 M ⁻¹

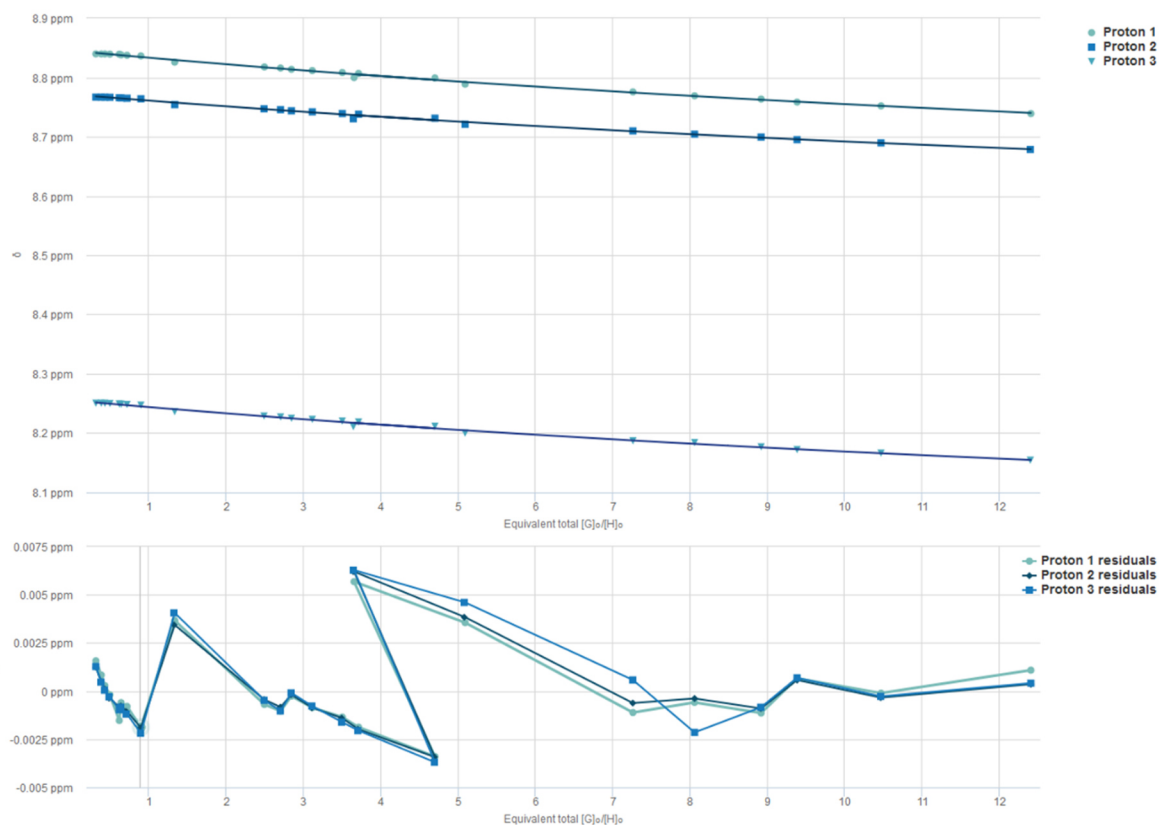


Figure S24: Assessment of the second measured titration data for the binding between Z-4 and 7. Top: plot of the chemical shift changes (¹H-NMR (400 MHz, 293 K, CD₂Cl₂)) of indicative protons H_a, H_b, and H_c of 7 occurring during the titration with Z-4 (dots, squares, and triangles) and nonlinear regression fit (*Bindfit* tool, solid lines). Bottom: deviation of the measured ¹H-NMR shifts from the fit.

Table S13: Chemical shifts of indicative protons H_a, H_b, and H_c of **7** observed in the ¹H-NMR spectra (400 MHz, 293 K, CDCl₃) during the first titration experiment. The concentration of **7** was kept constant while the concentration of **Z-4** was varied by irradiation with light of 405 nm or 470 nm wavelengths.

[7] in mol · L ⁻¹	[Z-4] in mol · L ⁻¹	δH _a	δH _b	δH _c
1.29E-03	4.21E-04	8.8410	8.7680	8.2510
1.29E-03	4.82E-04	8.8407	8.7677	8.2507
1.29E-03	5.36E-04	8.8402	8.7674	8.2504
1.29E-03	7.24E-04	8.8391	8.7667	8.2495
1.29E-03	7.41E-04	8.8391	8.7665	8.2495
1.29E-03	9.07E-04	8.8379	8.7655	8.2483
1.29E-03	1.13E-03	8.8366	8.7643	8.2470
1.29E-03	1.85E-03	8.8246	8.7527	8.2347
1.29E-03	2.05E-03	8.8231	8.7516	8.2334
1.29E-03	2.48E-03	8.8199	8.7487	8.2302
1.29E-03	3.01E-03	8.8165	8.7459	8.2274
1.29E-03	3.65E-03	8.8116	8.7425	8.2237
1.29E-03	4.69E-03	8.8065	8.7373	8.2180
1.29E-03	5.26E-03	8.8027	8.7341	8.2144
1.29E-03	5.86E-03	8.7993	8.7310	8.2118
1.29E-03	5.35E-03	8.7977	8.7282	8.2098
1.29E-03	6.03E-03	8.7902	8.7218	8.2006
1.29E-03	8.64E-03	8.7777	8.7111	8.1861
1.29E-03	1.02E-02	8.7688	8.7035	8.1810
1.29E-03	1.20E-02	8.7568	8.6933	8.1700
1.29E-03	1.34E-02	8.7525	8.6897	8.1659
1.29E-03	1.61E-02	8.7387	8.67785	8.1535

Table S14: Chemical shifts of indicative protons H_a, H_b, and H_c of **7** observed in the ¹H-NMR spectra (400 MHz, 293 K, CDCl₃) during the second titration experiment. The concentration of **7** was kept constant while the concentration of **Z-4** was varied by irradiation with light of 405 nm or 470 nm wavelengths.

[7] in mol · L ⁻¹	[Z-4] in mol · L ⁻¹	δH _a	δH _b	δH _c
1.29E-03	4.03E-04	8.8399	8.7671	8.2501
1.29E-03	4.93E-04	8.8398	8.7671	8.2501
1.29E-03	5.52E-04	8.8398	8.7670	8.2500
1.29E-03	6.37E-04	8.8395	8.7668	8.2496
1.29E-03	7.94E-04	8.8394	8.7660	8.2489
1.29E-03	8.24E-04	8.8382	8.7657	8.2485
1.29E-03	9.22E-04	8.8375	8.7652	8.2480
1.29E-03	1.15E-03	8.8365	8.7642	8.2470
1.29E-03	1.72E-03	8.8260	8.7545	8.2360
1.29E-03	3.21E-03	8.8179	8.7474	8.2286
1.29E-03	3.48E-03	8.8161	8.7459	8.2271
1.29E-03	3.67E-03	8.8139	8.7440	8.2248
1.29E-03	4.01E-03	8.8118	8.7423	8.2229
1.29E-03	4.51E-03	8.8085	8.7395	8.2201
1.29E-03	4.79E-03	8.8070	8.7383	8.2186
1.29E-03	6.06E-03	8.7994	8.7317	8.2115
1.29E-03	4.71E-03	8.8000	8.7306	8.2108
1.29E-03	6.56E-03	8.7890	8.7214	8.1999
1.29E-03	9.36E-03	8.7759	8.7102	8.1869
1.29E-03	1.04E-02	8.7694	8.7047	8.1839
1.29E-03	1.15E-02	8.7638	8.6998	8.1767
1.29E-03	1.21E-02	8.7588	8.6955	8.1721
1.29E-03	1.35E-02	8.7524	8.6901	8.1662
1.29E-03	1.60E-02	8.7394	8.679	8.1542

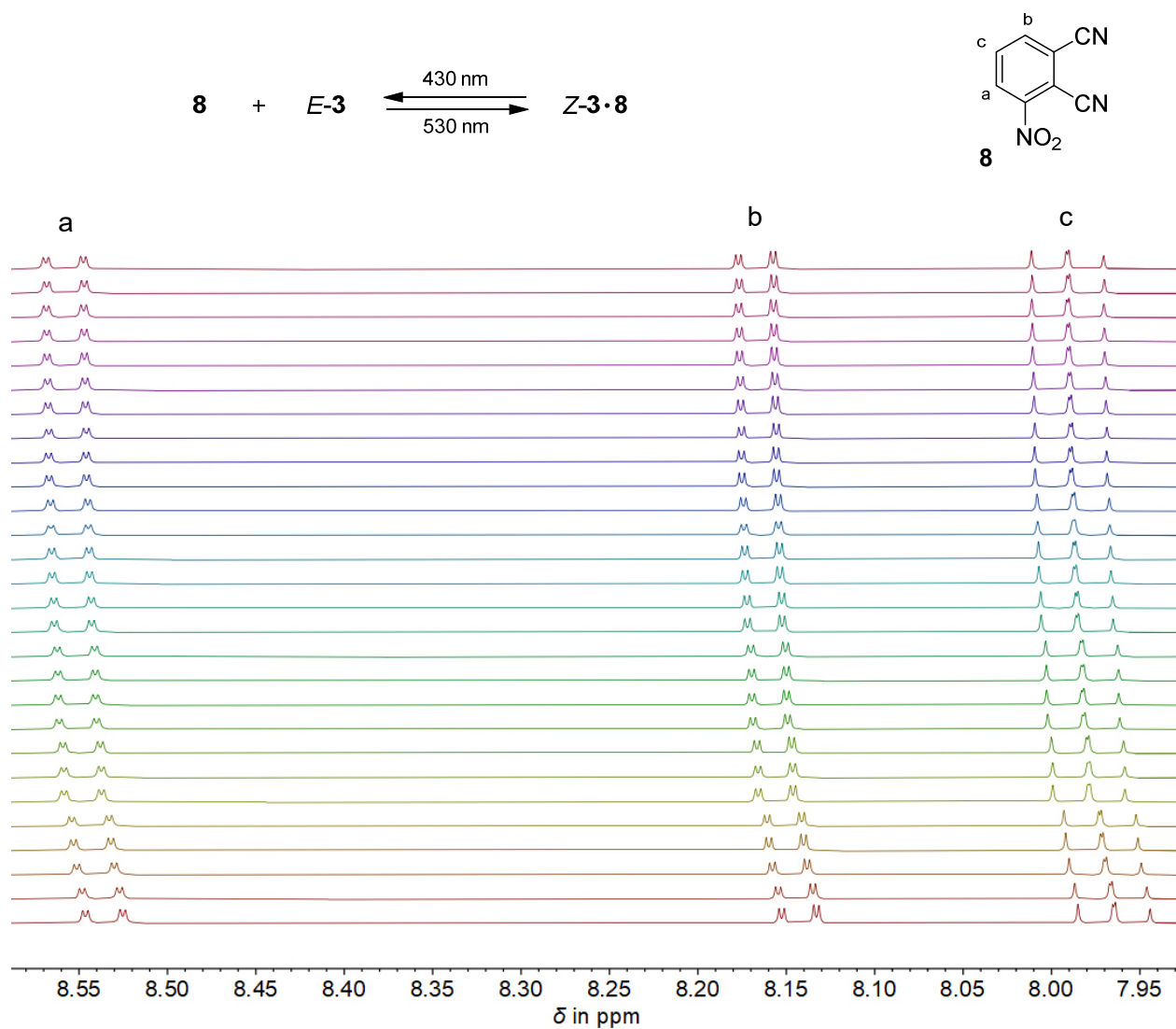


Figure S25: Determination of the binding constant K_a for formation of the association complex $Z\text{-}\mathbf{3}\cdot\mathbf{8}$ by NMR titration with the aid of light. One out of two independent experiments is shown exemplarily. Aromatic section of the ^1H -NMR spectra (400 MHz, 293 K, CD_2Cl_2) recorded during the titration showing the shift of indicative protons H_a , H_b , and H_c of **8**. The concentration of **8** was kept constant. Irradiation leads to varying E/Z isomer ratio of **3** resulting in varying ratios between **8** and binding $Z\text{-}\mathbf{3}$ (top highest $E\text{-}\mathbf{3}$ isomer content, bottom highest $Z\text{-}\mathbf{3}$ isomer content).

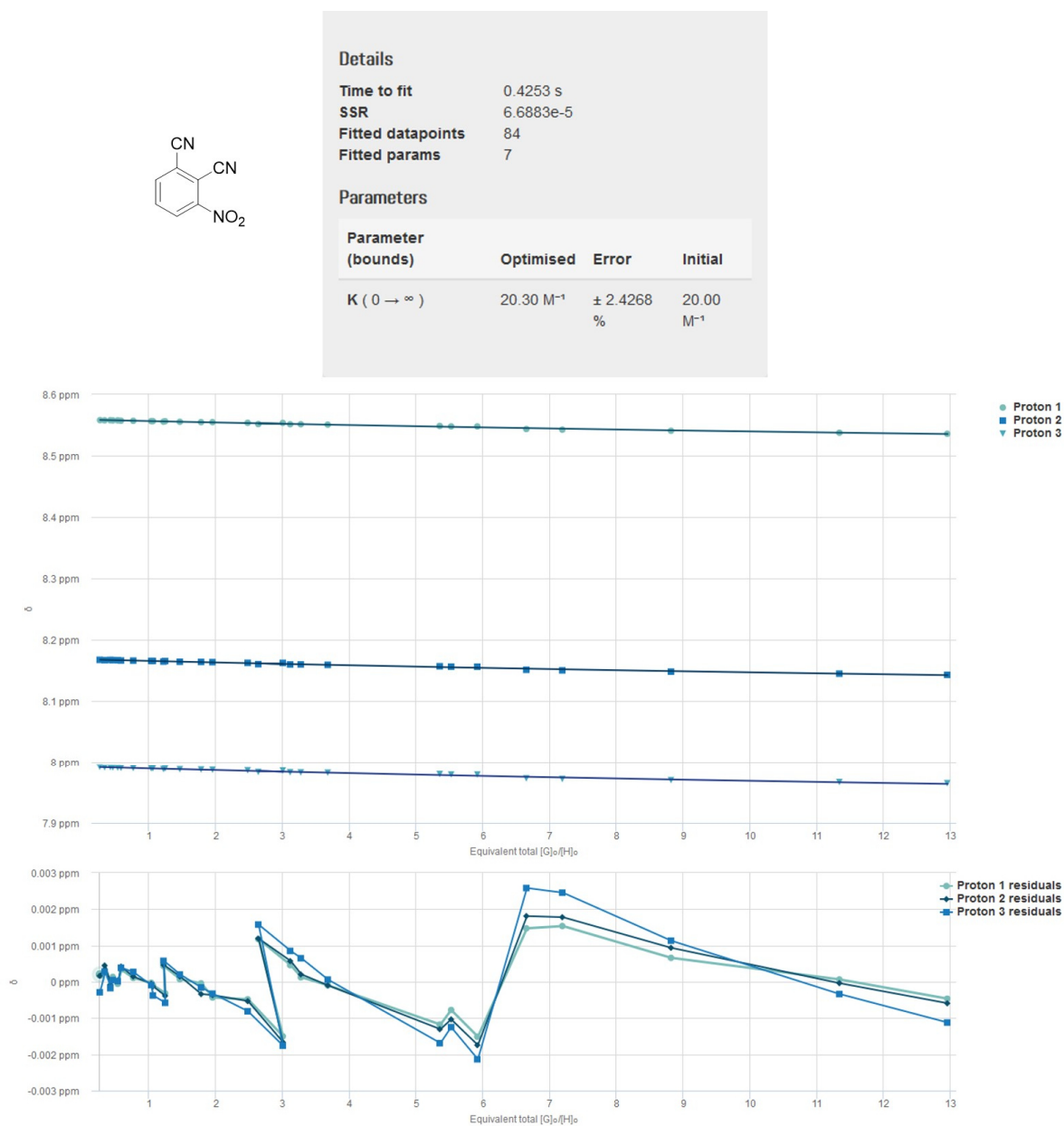


Figure S26: Assessment of the first measured titration data for the binding between **Z-3** and **8**. Top: plot of the chemical shift changes (¹H-NMR (400 MHz, 293 K, CD₂Cl₂)) of indicative protons H_a, H_b, and H_c of **8** occurring during the titration with **Z-3** (dots, squares, and triangles) and nonlinear regression fit (*Bindfit* tool, solid lines). Bottom: deviation of the measured ¹H-NMR shifts from the fit.



Figure S27: Assessment of the second measured titration data for the binding between **Z-3** and **8**. Top: plot of the chemical shift changes (¹H-NMR (400 MHz, 293 K, CD₂Cl₂)) of indicative protons H_a, H_b, and H_c of **8** occurring during the titration with **Z-3** (dots, squares, and triangles) and nonlinear regression fit (*Bindfit* tool, solid lines). Bottom: deviation of the measured ¹H-NMR shifts from the fit.

Table S15: Chemical shifts of indicative protons H_a, H_b, and H_c of **8** observed in the ¹H-NMR spectra (400 MHz, 293 K, CD₂Cl₂) during the first titration experiment. The concentration of **8** was kept constant while the concentration of Z-**3** was varied by irradiation with light of 430 nm or 530 nm wavelengths.

[8] in mol · L ⁻¹	[Z- 3] in mol · L ⁻¹	δH _a	δH _b	δH _c
1.44E-03	3.84E-04	8.5581	8.1673	7.9914
1.44E-03	5.00E-04	8.5578	8.1668	7.9906
1.44E-03	6.25E-04	8.5580	8.1671	7.9908
1.44E-03	6.63E-04	8.5577	8.1669	7.9905
1.44E-03	7.78E-04	8.5577	8.1667	7.9903
1.44E-03	8.43E-04	8.5572	8.1662	7.9898
1.44E-03	1.10E-03	8.5570	8.1660	7.9894
1.44E-03	1.49E-03	8.5565	8.1655	7.9890
1.44E-03	1.54E-03	8.5565	8.1655	7.9892
1.44E-03	1.79E-03	8.5563	8.1653	7.9889
1.44E-03	1.77E-03	8.5556	8.1645	7.9878
1.44E-03	2.12E-03	8.5554	8.1642	7.9875
1.44E-03	2.57E-03	8.5548	8.1639	7.9870
1.44E-03	2.83E-03	8.5548	8.1635	7.9867
1.44E-03	3.58E-03	8.5537	8.1624	7.9858
1.44E-03	4.34E-03	8.5536	8.1623	7.9854
1.44E-03	3.81E-03	8.5517	8.1603	7.9830
1.44E-03	4.50E-03	8.5514	8.1598	7.9825
1.44E-03	4.74E-03	8.5514	8.1598	7.9823
1.44E-03	5.31E-03	8.5508	8.1592	7.9819
1.44E-03	7.74E-03	8.5486	8.1568	7.9797
1.44E-03	7.97E-03	8.5479	8.1562	7.9789
1.44E-03	8.55E-03	8.5479	8.1561	7.9789
1.44E-03	9.61E-03	8.5436	8.1511	7.9726
1.44E-03	1.04E-02	8.5426	8.1501	7.9716
1.44E-03	1.27E-02	8.5408	8.1480	7.9697
1.44E-03	1.64E-02	8.5376	8.1448	7.9666
1.44E-03	1.87E-02	8.5359	8.1429	7.9647

Table S16: Chemical shifts of indicative protons H_a, H_b, and H_c of **8** observed in the ¹H-NMR spectra (400 MHz, 293 K, CD₂Cl₂) during the second titration experiment. The concentration of **8** was kept constant while the concentration of **Z-3** was varied by irradiation with light of 430 nm or 530 nm wavelengths.

[8] in mol · L ⁻¹	[Z-3] in mol · L ⁻¹	δH _a	δH _b	δH _c
1.44E-03	3.91E-04	8.5579	8.1671	7.9907
1.44E-03	4.89E-04	8.5579	8.1669	7.9906
1.44E-03	6.57E-04	8.5576	8.1668	7.9904
1.44E-03	8.19E-04	8.5576	8.1666	7.9903
1.44E-03	7.57E-04	8.557	8.1660	7.9895
1.44E-03	9.51E-04	8.5567	8.1657	7.9894
1.44E-03	1.02E-03	8.5567	8.1657	7.9892
1.44E-03	1.49E-03	8.5564	8.1652	7.9889
1.44E-03	1.86E-03	8.5558	8.1648	7.9884
1.44E-03	1.77E-03	8.5554	8.1643	7.9876
1.44E-03	2.57E-03	8.5548	8.1635	7.9869
1.44E-03	3.03E-03	8.5545	8.1631	7.9865
1.44E-03	3.43E-03	8.5539	8.1627	7.9860
1.44E-03	3.88E-03	8.5533	8.1620	7.9854
1.44E-03	3.93E-03	8.552	8.1604	7.9831
1.44E-03	4.74E-03	8.5512	8.1596	7.9823
1.44E-03	5.89E-03	8.5501	8.1585	7.9812
1.44E-03	8.09E-03	8.5486	8.1567	7.9795
1.44E-03	9.82E-03	8.547	8.1549	7.9778
1.44E-03	1.01E-02	8.5426	8.1501	7.9716
1.44E-03	1.30E-02	8.5403	8.1476	7.9692
1.44E-03	1.45E-02	8.5389	8.1462	7.9678
1.44E-03	1.67E-02	8.537	8.1439	7.9656
1.44E-03	2.28E-02	8.532	8.1386	7.9604

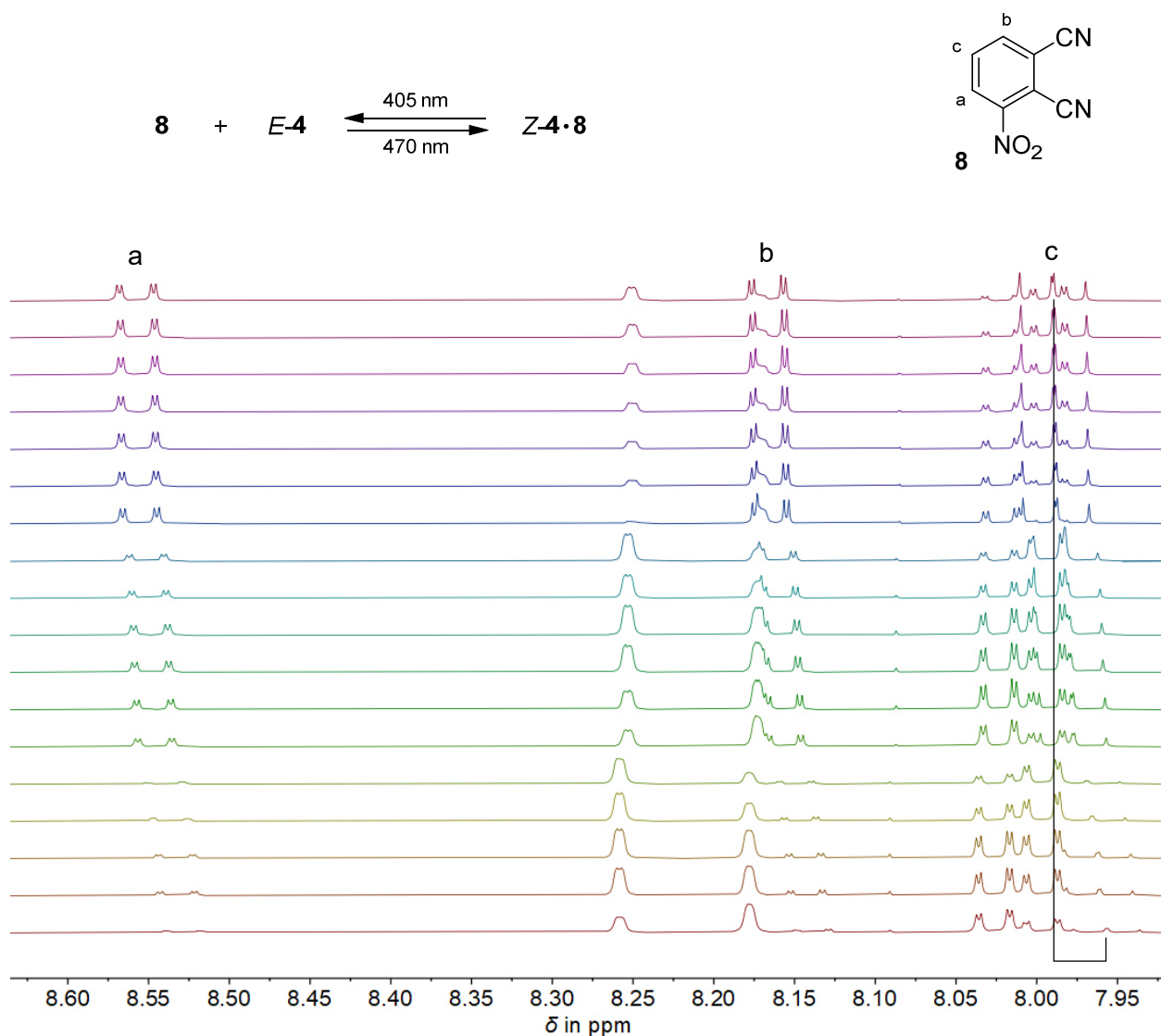


Figure S28: Determination of the binding constant K_a for formation of the association complex $Z\text{-}\mathbf{4} \cdot \mathbf{8}$ by NMR titration with the aid of light. One out of two independent experiments is shown exemplarily. Aromatic section of the ^1H -NMR spectra (400 MHz, 293 K, CD_2Cl_2) recorded during the titration showing the shift of indicative protons H_a , H_b , and H_c of **8**. The concentration of **8** was kept constant. Irradiation leads to varying E/Z isomer ratio of **4** resulting in varying ratios between **8** and binding $Z\text{-}\mathbf{4}$ (top highest $E\text{-}\mathbf{4}$ isomer content, bottom highest $Z\text{-}\mathbf{4}$ isomer content).

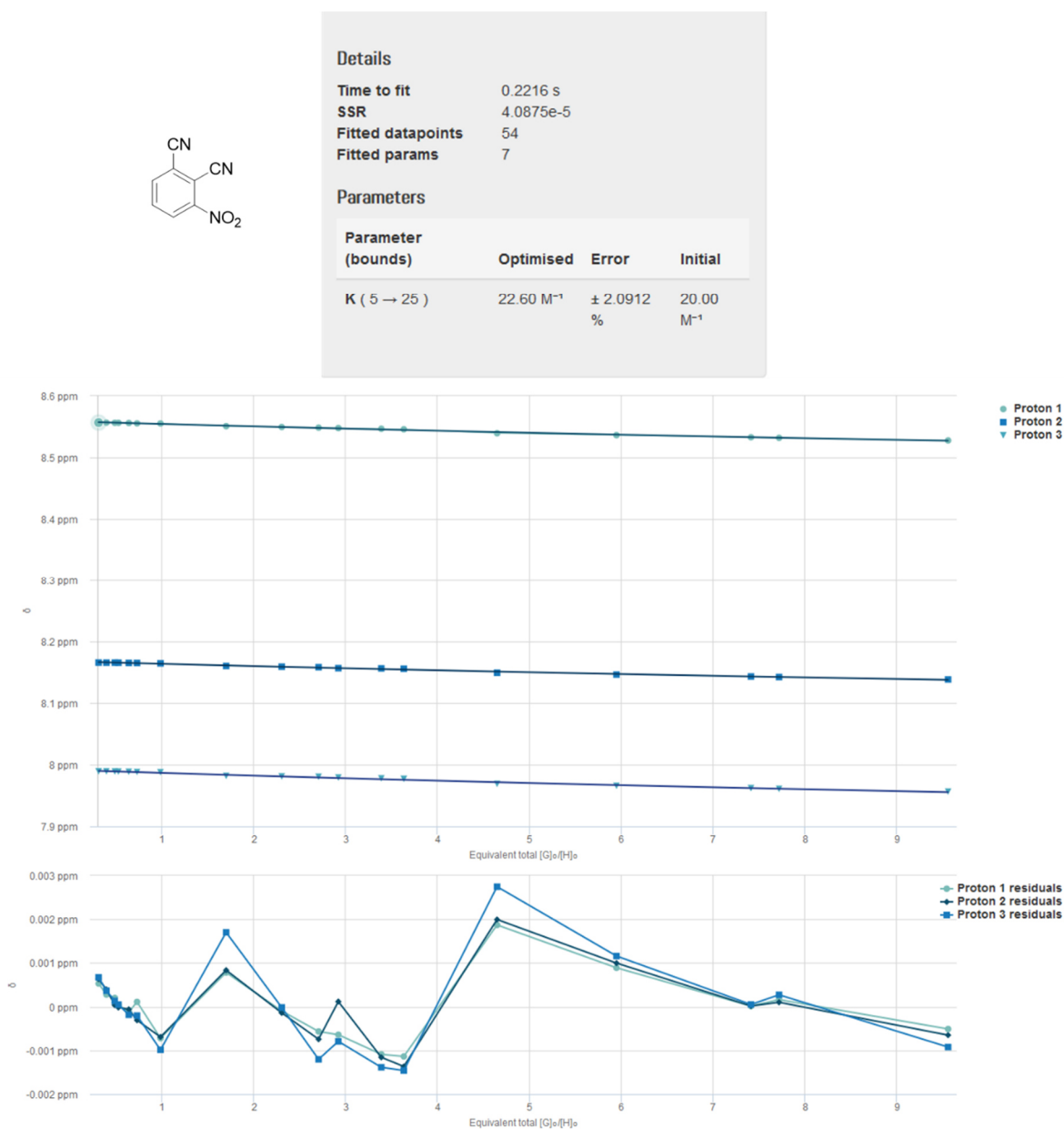


Figure S29: Assessment of the first measured titration data for the binding between **Z-4** and **8**. Top: plot of the chemical shift changes (¹H-NMR (400 MHz, 293 K, CD₂Cl₂)) of indicative protons H_a, H_b, and H_c of **8** occurring during the titration with **Z-4** (dots, squares, and triangles) and nonlinear regression fit (*Bindfit* tool, solid lines). Bottom: deviation of the measured ¹H-NMR shifts from the fit.

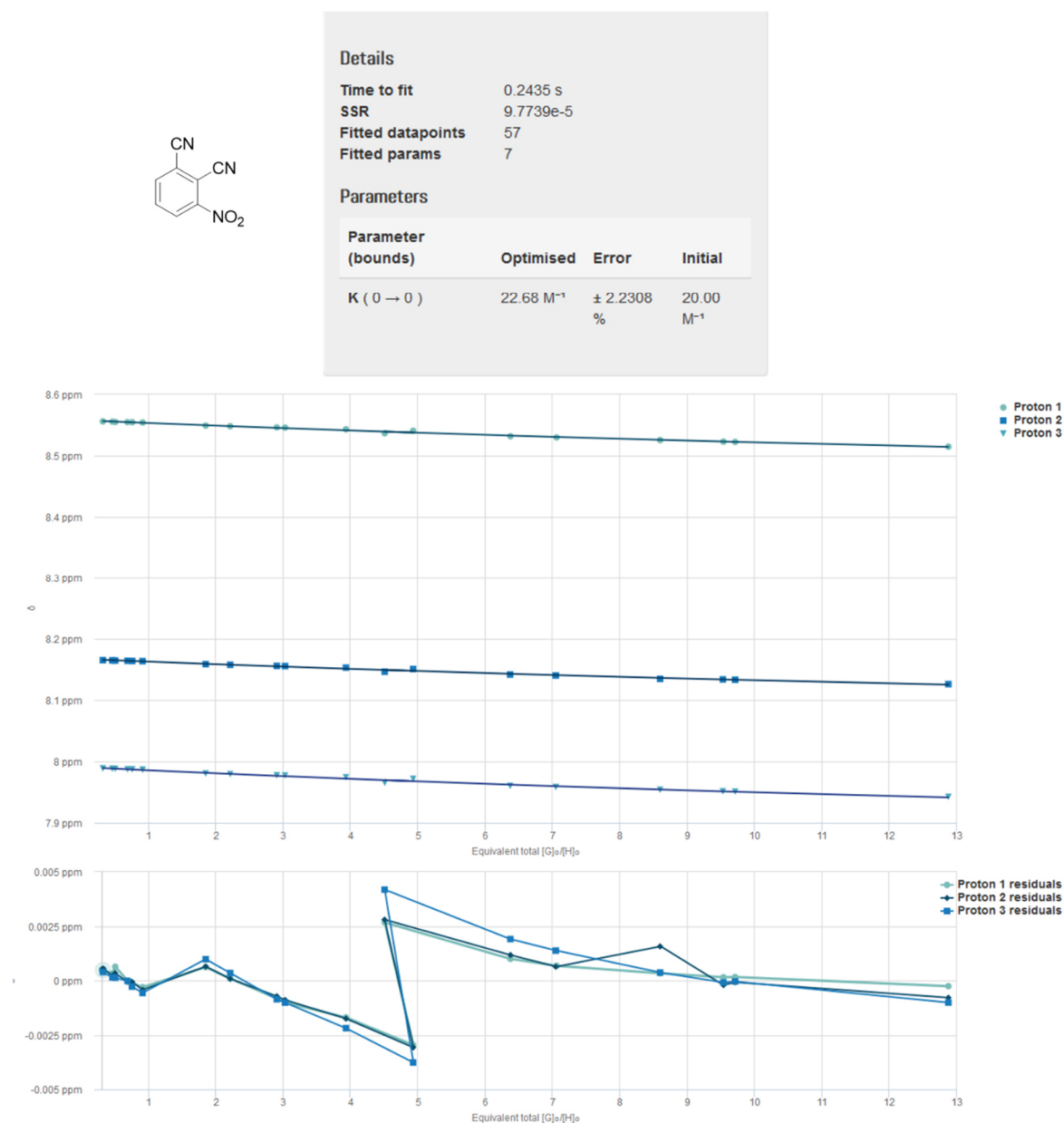


Figure S30: Assessment of the second measured titration data for the binding between **Z-4** and **8**. Top: plot of the chemical shift changes (¹H-NMR (400 MHz, 293 K, CD₂Cl₂)) of indicative protons H_a, H_b, and H_c of **8** occurring during the titration with **Z-4** (dots, squares, and triangles) and nonlinear regression fit (*Bindfit* tool, solid lines). Bottom: deviation of the measured ¹H-NMR shifts from the fit.

Table S17: Chemical shifts of indicative protons H_a, H_b, and H_c of **8** observed in the ¹H-NMR spectra (400 MHz, 293 K, CD₂Cl₂) during the first titration experiment. The concentration of **8** was kept constant while the concentration of Z-**4** was varied by irradiation with light of 405 nm or 470 nm wavelengths.

[8] in mol · L ⁻¹	[Z- 4] in mol · L ⁻¹	δH _a	δH _b	δH _c
1.44E-03	4.44E-04	8.5567	8.1658	7.9893
1.44E-03	5.66E-04	8.5566	8.1657	7.9892
1.44E-03	6.98E-04	8.5563	8.1657	7.9890
1.44E-03	7.54E-04	8.5563	8.1656	7.9889
1.44E-03	9.17E-04	8.556	8.1652	7.9886
1.44E-03	1.05E-03	8.5554	8.1651	7.9882
1.44E-03	1.41E-03	8.5552	8.1645	7.9878
1.44E-03	2.44E-03	8.5509	8.1603	7.9819
1.44E-03	3.31E-03	8.5495	8.1591	7.9810
1.44E-03	3.89E-03	8.5485	8.1583	7.9805
1.44E-03	4.20E-03	8.5478	8.1567	7.9792
1.44E-03	4.88E-03	8.5466	8.1564	7.9779
1.44E-03	5.23E-03	8.5458	8.1558	7.9770
1.44E-03	6.69E-03	8.5394	8.1492	7.9689
1.44E-03	8.56E-03	8.5363	8.1463	7.9658
1.44E-03	1.07E-02	8.5329	8.1432	7.9620
1.44E-03	1.11E-02	8.5319	8.1423	7.9608
1.44E-03	1.38E-02	8.5277	8.1384	7.9564

Table S18: Chemical shifts of indicative protons H_a, H_b, and H_c of **8** observed in the ¹H-NMR spectra (400 MHz, 293 K, CD₂Cl₂) during the second titration experiment. The concentration of **8** was kept constant while the concentration of Z-4 was varied by irradiation with light of 405 nm or 470 nm wavelengths.

[7] in mol · L ⁻¹	[Z-4] in mol · L ⁻¹	δH _a	δH _b	δH _c
1.44E-03	4.59E-04	8.556	8.1652	7.9888
1.44E-03	6.63E-04	8.5555	8.1649	7.9883
1.44E-03	7.23E-04	8.555	8.1646	7.9881
1.44E-03	9.86E-04	8.5548	8.1642	7.9873
1.44E-03	1.09E-03	8.5546	8.1639	7.9872
1.44E-03	1.31E-03	8.5541	8.1636	7.9867
1.44E-03	2.66E-03	8.5491	8.1586	7.9805
1.44E-03	3.18E-03	8.5481	8.1577	7.9794
1.44E-03	4.18E-03	8.5462	8.1558	7.9774
1.44E-03	4.36E-03	8.5459	8.1555	7.9770
1.44E-03	5.66E-03	8.5431	8.1530	7.9742
1.44E-03	7.10E-03	8.5407	8.1508	7.9716
1.44E-03	6.49E-03	8.5366	8.1464	7.9654
1.44E-03	9.17E-03	8.5318	8.1418	7.9603
1.44E-03	1.02E-02	8.5299	8.1402	7.9583
1.44E-03	1.24E-02	8.5255	8.1347	7.9539
1.44E-03	1.37E-02	8.523	8.1339	7.9513
1.44E-03	1.40E-02	8.5225	8.1333	7.9507
1.44E-03	1.85E-02	8.5147	8.1261	7.9423

Summary of the binding parameters for complexes of Z-4 with guest molecules 5 - 8

Table S19: Measured binding constants K_a for the association between tweezers Z-3 or Z-4 and guest molecules 5-8. K_a values were obtained from experimental chemical shifts using nonlinear regression fits (*Bindfit* online tool). * Taken from Ref. 1.

Guest	K_a in L mol ⁻¹		K_a in L mol ⁻¹	
	with Z-3 (Temperature)	Solvent	with Z-4 (Temperature)	Solvent
DTF (5)	2376 (253 K)*	CDCl ₃	4136 (253 K)*	CDCl ₃
			1833 (273 K)*	CDCl ₃
			1160 (293 K)*	CDCl ₃
			1020 (293 K)	CDCl ₃
TCNB (6)	11.88 (293 K)	CD ₂ Cl ₂	26.12 (293 K)	CD ₂ Cl ₂
	8.89 (293 K)	CD ₂ Cl ₂	24.85 (293 K)	CD ₂ Cl ₂
PhA (7)	14.24 (293 K)	CDCl ₃	39.63 (293 K)	CDCl ₃
	16.92 (293 K)	CDCl ₃	30.21 (293 K)	CDCl ₃
3NPN (8)	20.30 (293 K)	CD ₂ Cl ₂	22.60 (293 K)	CD ₂ Cl ₂
	17.02 (293 K)	CD ₂ Cl ₂	22.68 (293 K)	CD ₂ Cl ₂

Theoretical description of **4** and the **Z-4·5** complex

All calculations were performed with the Gaussian16 Revision A.03⁴ program package. **5**, *E-4*, and *Z-4* were optimized on the B3LYP/6-311G(d,p) IEFPCM (CHCl₃) level of theory and have been confirmed to be minimum structures by frequency analysis. Based on the B3LYP/6-311G(d,p) optimized structures electrostatic potentials (ESPs) for *E-4*, *Z-4*, and **5** were calculated and visualized using GaussView 5.0.8.

For the calculations of the **Z-4·5** complex structure only the (*S*) enantiomer of **4** was considered. For the complex structure **Z-4·5** dispersion forces between **4** and **5** have been included in the calculation by using D3 Grimme-dispersion with Becke-Johnson damping (GD3BJ).

For the calculation of the **Z-4·5** complex different orientations of **5** within the binding pocket of *Z-4* were considered. Therefore a MM3* force field method with Monte Carlo Multiple Minimum (MCMM) search algorithm with a threshold of 8 kJ/mol was used to find starting structures for DFT optimization. The resulting three geometries were complemented with two geometries created manually. The geometries were further optimized on the B3LYP GD3BJ/6311G(d,p) IEFPCM (CHCl₃) level of theory. Frequency analysis of the complex structures were omitted, because they are cost intensive and often produce one or more imaginary frequencies due to numerical noise.⁵

The resulting DFT optimized structures are shown below in Figure S31 together with their relative energy differences.

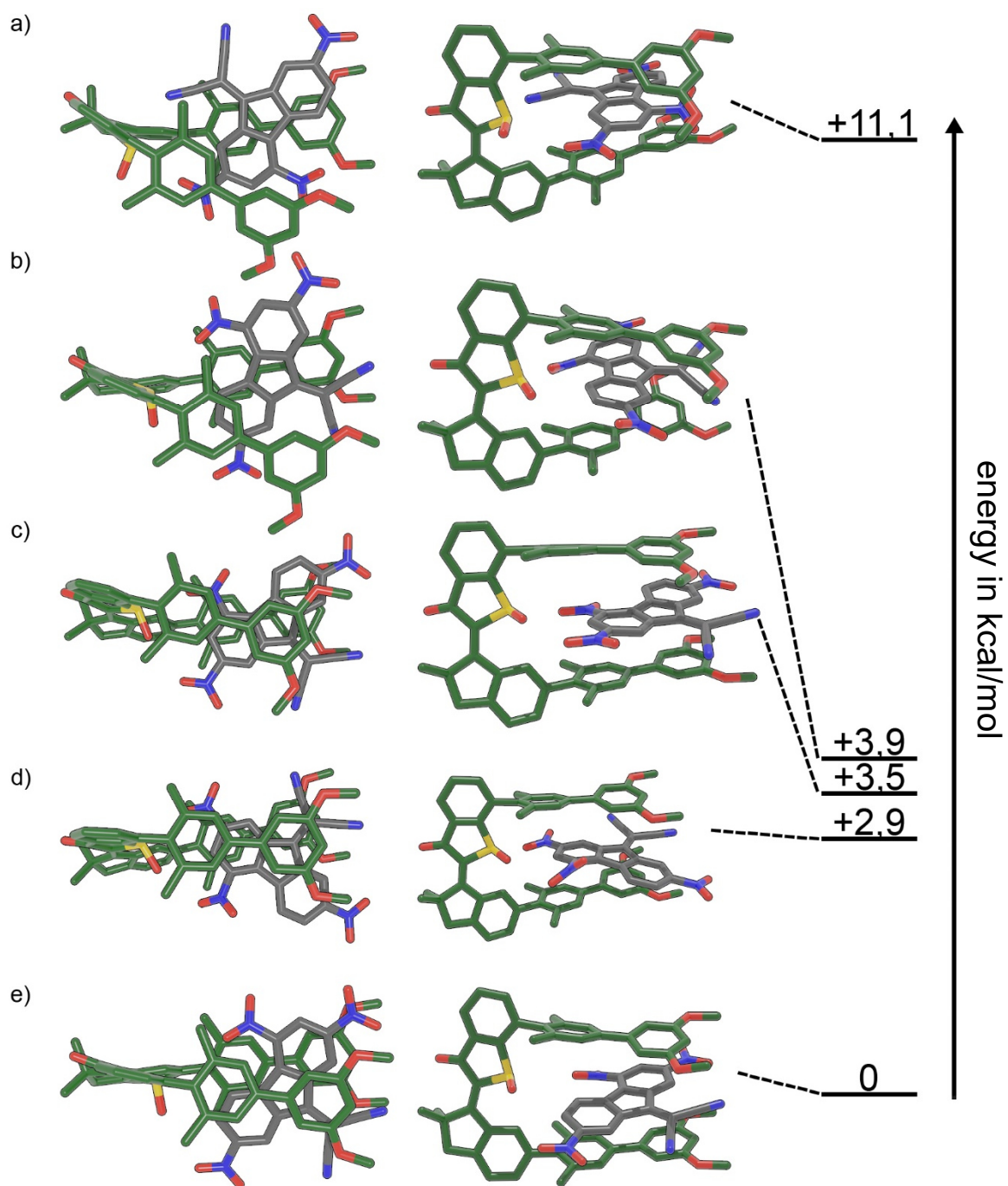


Figure S31: Optimized minimum structures of the association complex between Z-4 and guest 5. Different complex geometries were assessed and ranked according to their relative energies a) to e).

NMR spectra

^1H and ^{13}C NMR spectra of **4**

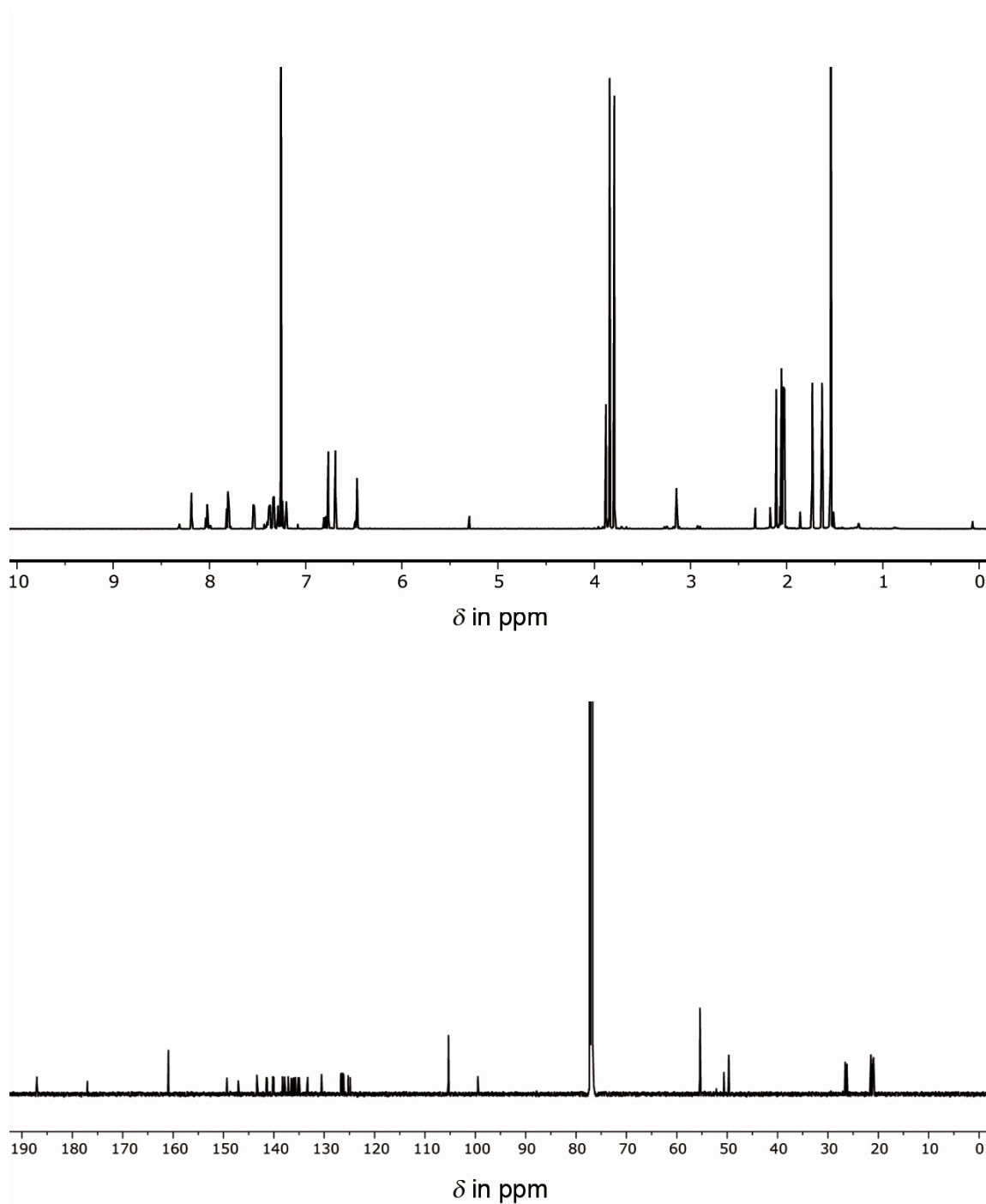


Figure S32 ^1H -NMR spectrum (600 MHz, 293 K, CDCl_3 , top) and ^{13}C -NMR spectrum (150 MHz, 293 K, CDCl_3 , bottom) of a 87:13 mixture of *Z*:*E* isomers of **4**.

Crystal structural data

Experimental details

The X-ray intensity data of Z-4 (yv439) were measured on a Bruker D8 Venture TXS system equipped with a multilayer mirror monochromator and a Mo K α rotating anode X-ray tube ($\lambda = 0.71073 \text{ \AA}$). The frames were integrated with the Bruker SAINT software package.⁶ Data were corrected for absorption effects using the Multi-Scan method (SADABS).⁷ The structure was solved and refined using the Bruker SHELXTL Software Package.⁸ All hydrogen atoms have been calculated in ideal geometry riding on their parent atoms. The disorder of the S-bound O has been described by a split model. The ratio of site occupation factors of the two O atoms refined to 0.91/0.09. The minor part has been refined isotropically. The structure has been refined as a 2-component inversion twin, BASF refined to 0.25. The solvent could not be modelled properly and has been squeezed out. According to PLATON SQUEEZE⁹ there are four voids each with a volume of 162 \AA^3 and 47 squeezed-out electrons. This corresponds to 1.5 Acetone in each of these voids. The figures have been drawn at the 50% ellipsoid probability level.¹⁰ The less-occupied moieties of disordered parts have been omitted for the figures.

Compound	Z-4 (CCDC 2031007)
net formula	C ₅₁ H ₄₈ O ₆ S
M_r /g mol ⁻¹	788.95
crystal size/mm	0.100 × 0.030 × 0.030
T /K	102.(2)
radiation	MoK α
diffractometer	'Bruker D8 Venture TXS'
crystal system	orthorhombic
space group	'P 21 21 21'
a /Å	8.0941(8)
b /Å	17.5936(15)
c /Å	32.602(3)
α /°	90
β /°	90
γ /°	90
V /Å ³	4642.7(7)
Z	4
calc. density/g cm ⁻³	1.129
μ /mm ⁻¹	0.116
absorption correction	Multi-Scan
transmission factor	0.93–1.00
refls. measured	55923
R_{int}	0.0974
mean $\sigma(I)/I$	0.0650
θ range	2.979–25.347
observed refls.	6654
x, y (weighting)	0.0676, 0.9140
hydrogen refinement	constr
Flack parameter	0.25(13)
refls in refinement	8495
parameters	539
restraints	0
$R(F_{\text{obs}})$	0.0526
$R_w(F^2)$	0.1335
S	1.058
shift/error _{max}	0.001
max electron density/e	0.204
min electron density/e	-0.431

Calculated ground state minima geometries - xyz coordinates

(S)-E-4				(S)-Z-4			
C	0.4497600	12.234.281	-10.491.191	C	-48.680.884	-0.5826710	0.3145010
C	-0.0255260	24.138.602	-0.5801240	C	-49.394.004	-17.759.931	-0.3455210
C	-0.3033910	0.0391680	-15.535.891	C	-59.508.794	0.1765740	0.9906431
C	0.8493471	36.283.903	-0.1586260	C	-62.315.165	-25.171.592	-0.7753591
S	22.547.112	0.8467011	-10.575.791	S	-32.888.122	0.3540860	0.3866960
C	0.5413420	-11.799.461	-14.604.591	C	-55.336.724	15.863.561	12.078.531
O	-14.389.971	0.0273560	-19.959.721	O	-70.288.525	-0.2635410	13.562.531
C	-0.1689030	48.038.803	-0.0968230	C	-57.339.494	-34.459.212	-19.289.011
C	19.879.811	40.095.463	-11.214.731	C	-73.652.635	-16.248.831	-13.074.731
C	14.098.331	33.658.112	12.604.341	C	-67.280.515	-33.813.042	0.4079200
C	-15.061.401	41.482.373	0.0196750	C	-42.530.133	-35.419.053	-17.414.791
C	18.602.591	-0.9290921	-11.028.731	C	-42.113.983	18.463.701	0.8679641
O	28.547.002	11.579.451	-24.242.862	O	-24.778.542	-0.0528920	16.152.101
C	0.1022780	-24.841.692	-16.708.321	C	-63.520.714	26.056.302	16.867.781
H	-0.1169550	53.929.204	-10.192.831	H	-59.642.024	-29.923.862	-28.991.852
H	0.0462760	54.859.594	0.7298571	H	-62.279.204	-44.209.413	-19.073.751
H	23.583.932	50.002.214	-0.8414261	H	-81.116.506	-22.617.242	-17.916.871
H	16.346.761	40.586.993	-21.536.582	H	-69.919.565	-0.9220081	-20.576.471
H	28.356.592	33.280.222	-10.896.091	H	-78.602.186	-10.677.341	-0.5172380
H	20.937.101	25.157.882	12.609.251	H	-70.139.635	-27.477.262	12.468.741
H	19.607.981	42.454.243	16.043.141	H	-76.005.785	-39.612.623	0.0936710
H	0.6066730	31.647.922	19.739.261	H	-59.555.574	-40.803.193	0.7391121
C	28.038.592	-19.430.021	-0.9460591	C	-36.388.863	31.120.152	0.9830481
C	10.161.501	-35.207.243	-15.046.881	C	-58.126.664	38.831.693	18.054.341
H	-0.9281161	-26.686.662	-19.499.811	H	-73.804.105	23.915.602	19.519.691
C	23.404.992	-32.528.362	-11.472.441	C	-44.816.653	41.294.473	14.579.351
H	0.7028371	-45.475.663	-16.520.831	H	-64.267.415	46.987.303	21.688.662
H	30.365.502	-40.749.873	-10.234.361	H	-40.807.133	51.320.664	15.562.741
C	-14.283.121	27.796.672	-0.2919120	C	-38.011.913	-25.705.292	-0.8322601
C	-25.876.672	19.904.861	-0.2003750	C	-24.433.542	-25.329.652	-0.4678190
H	-25.583.502	0.9371371	-0.4247100	H	-20.850.991	-18.640.891	0.3041810
C	-38.029.553	25.635.572	0.1707290	C	-15.400.571	-34.175.122	-10.590.391
C	-38.571.933	39.400.923	0.4502410	C	-20.098.941	-43.513.533	-19.979.981
H	-48.061.433	43.868.913	0.7264321	H	-13.051.511	-50.376.184	-24.550.152
C	-27.155.492	47.312.413	0.3813860	C	-33.600.342	-44.280.993	-23.304.652
H	-27.681.722	57.894.434	0.6127460	H	-37.070.083	-51.746.454	-30.364.282
C	42.317.123	-16.752.431	-0.5839510	C	-22.132.172	33.944.292	0.6231550
C	51.987.314	-15.450.701	-16.000.261	C	-12.128.781	33.210.062	16.121.501
C	46.056.013	-15.803.281	0.7705891	C	-18.832.531	37.546.233	-0.6978011
C	65.287.735	-13.251.481	-12.389.031	C	0.1046560	36.166.833	12.597.901
C	59.457.934	-13.572.491	10.881.571	C	-0.5532870	40.398.463	-10.083.231
C	69.264.665	-12.290.051	0.0986650	C	0.4584980	39.791.393	-0.0440750

H	72.668.345	-12.017.051	-20.233.291	H	0.8760031	35.345.053	20.170.421
H	62.331.535	-13.076.411	21.324.042	H	-0.3068240	43.384.413	-20.210.001
C	-50.394.404	17.216.021	0.2576330	C	-0.0892020	-33.882.112	-0.6852841
C	-55.129.184	12.851.461	15.105.271	C	0.4136470	-42.988.963	0.2641480
C	-57.292.844	13.631.791	-0.9176391	C	0.7736501	-24.519.902	-12.876.031
C	-66.658.835	0.5003470	15.677.221	C	17.699.431	-42.613.563	0.5909610
C	-68.817.025	0.5817920	-0.8185051	C	21.247.882	-24.485.812	-0.9373781
C	-73.695.126	0.1370730	0.4147090	C	26.469.232	-33.458.062	0.0000850
H	-70.329.885	0.1820130	25.371.632	H	21.530.762	-49.775.504	13.093.051
H	-73.970.125	0.2953560	-17.285.871	H	27.787.012	-17.116.021	-13.899.611
C	83.508.636	-0.9978171	0.4588140	C	18.698.371	42.888.643	-0.3964440
C	93.728.817	-16.125.051	-0.2722580	C	26.883.952	49.789.354	0.5038670
C	86.828.586	-0.1642090	15.320.271	C	23.934.102	38.918.603	-16.314.911
C	107.090.378	-13.944.501	0.0679150	C	40.134.403	52.653.404	0.1712650
H	91.533.886	-22.828.552	-10.929.561	H	23.115.012	53.226.774	14.582.331
C	100.208.607	0.0505430	18.670.331	C	37.192.133	41.811.413	-19.583.751
H	79.204.076	0.3493990	21.029.202	H	17.986.901	33.322.622	-23.415.082
C	110.489.638	-0.5613950	11.403.251	C	45.445.123	48.703.594	-10.621.711
H	120.819.769	-0.3941090	14.010.351	H	55.690.324	50.914.944	-13.160.181
C	-85.974.576	-0.6981381	0.4967340	C	40.903.683	-33.274.562	0.3582590
C	-96.803.597	-0.4489090	-0.3533190	C	50.590.224	-30.792.732	-0.6204400
C	-86.824.876	-17.426.771	14.236.721	C	44.955.423	-35.597.113	16.770.871
C	-108.307.628	-12.356.641	-0.2758660	C	64.128.665	-30.635.482	-0.2817780
H	-96.610.037	0.3659480	-10.651.921	H	47.853.653	-29.193.712	-16.551.781
C	-98.358.147	-25.255.502	14.969.691	C	58.511.014	-35.440.013	20.093.801
H	-78.555.715	-19.820.551	20.794.771	H	37.741.663	-37.272.743	24.661.532
C	-109.227.548	-22.823.332	0.6491010	C	68.255.085	-32.959.272	10.354.331
H	-118.125.369	-28.888.862	0.7068121	H	78.722.466	-32.838.652	12.945.041
C	48.158.333	-16.109.591	-30.596.242	C	-15.389.751	28.965.402	30.241.412
H	41.040.583	-0.8176741	-33.058.852	H	-19.361.041	18.771.611	30.299.792
H	43.446.303	-25.658.692	-33.101.902	H	-22.908.572	35.479.213	34.789.872
H	56.957.584	-14.927.161	-36.938.743	H	-0.6458530	29.219.042	36.503.443
C	35.882.243	-17.245.021	18.791.051	C	-29.376.792	38.390.103	-17.775.531
H	30.658.832	-26.838.702	18.259.191	H	-37.420.323	45.283.483	-15.064.611
H	28.238.382	-0.9435231	18.251.291	H	-34.010.332	28.642.952	-19.588.181
H	40.688.603	-16.547.541	28.559.092	H	-25.013.352	41.805.443	-27.172.572
C	-47.948.543	16.452.981	27.917.112	C	-0.4868340	-53.103.184	0.9365071
H	-48.262.903	27.215.512	29.851.302	H	-0.9129631	-60.151.925	0.2166110
H	-37.393.533	13.625.321	27.511.282	H	-13.274.641	-48.236.993	14.388.271
H	-52.500.364	11.390.341	36.444.973	H	0.0664290	-58.845.444	16.813.531
C	-52.441.524	18.047.751	-22.800.092	C	0.2637490	-14.507.361	-22.993.882
H	-42.701.033	13.701.351	-25.206.772	H	-0.4616430	-0.7637631	-18.543.641
H	-51.268.614	28.909.732	-23.300.742	H	-0.2388750	-19.459.191	-31.352.072
H	-59.492.184	15.030.331	-30.562.502	H	10.855.111	-0.8558621	-27.010.172
O	-98.124.947	-35.224.743	24.280.052	O	61.379.734	-37.746.443	33.230.652
O	-118.302.168	-0.9043501	-11.431.651	O	72.750.305	-28.202.872	-13.113.901
O	102.362.857	0.8868821	29.228.052	O	41.328.473	37.425.613	-31.820.542

O	116.262.319	-20.476.691	-0.7016280	O	47.226.493	59.491.274	11.147.301
C	-130.414.919	-16.544.861	-11.160.631	C	86.743.376	-27.960.192	-10.448.241
H	-128.653.679	-27.083.422	-13.547.241	H	89.328.077	-20.049.741	-0.3333430
H	-136.785.800	-12.147.861	-18.811.281	H	91.538.677	-25.905.142	-20.000.741
H	-135.384.980	-15.770.051	-0.1436100	H	90.266.306	-37.602.323	-0.6640411
C	-109.486.338	-43.733.983	25.535.502	C	74.987.825	-37.538.493	37.445.053
H	-107.017.818	-50.815.044	33.423.602	H	74.798.465	-39.523.603	48.144.553
H	-111.437.468	-49.202.334	16.253.561	H	79.580.946	-27.760.462	35.666.323
H	-118.417.408	-38.092.823	28.413.142	H	80.855.496	-45.308.763	32.437.242
C	130.115.710	-18.819.781	-0.4113560	C	60.829.565	62.788.054	0.8476891
H	133.199.859	-0.8367441	-0.5153200	H	66.908.345	53.802.724	0.7005471
H	135.414.060	-24.872.322	-11.444.541	H	64.363.765	68.113.095	17.286.521
H	132.549.820	-22.380.232	0.5949660	H	61.728.224	69.296.825	-0.0281360
C	115.770.178	11.698.001	33.143.172	C	54.823.154	39.751.583	-35.761.823
H	115.005.078	18.526.141	41.583.783	H	55.810.984	35.344.173	-45.664.113
H	121.358.529	16.541.541	25.070.522	H	61.873.644	34.908.233	-28.930.072
H	121.017.709	0.2624210	36.303.503	H	57.042.754	50.457.674	-36.340.043
Z-4·5				5			
C	-46.846.616	26.360.237	-0.1602141	C	30.626.909	-12.530.992	0.0309204
O	-79.273.829	15.532.867	-11.118.997	C	32.941.373	0.1100014	0.0517696
C	-37.963.105	36.894.083	0.0304684	C	22.642.994	10.436.010	0.0197279
C	-65.424.364	41.096.413	-0.5797260	C	0.9587866	0.5724276	-0.0263490
C	-56.883.846	51.849.940	-0.3579572	C	0.6694120	-0.8203172	-0.0573014
C	-43.370.914	49.775.159	-0.0624932	C	17.495.574	-17.059.175	-0.0436618
C	-60.256.813	28.216.683	-0.4641832	H	38.852.479	-19.519.695	0.0647409
C	-67.797.283	15.641.524	-0.6933612	H	25.140.352	20.926.656	0.0405126
C	-59.167.418	0.3867212	-0.4346846	C	-13.804.514	0.3114693	-0.0173287
C	-62.410.720	-0.9371037	-0.4001599	C	-27.615.774	0.4645960	0.0317423
C	-76.687.499	-15.262.896	-0.3954433	C	-35.366.888	-0.6892066	0.0713224
C	-39.411.707	-44.919.613	-0.2594923	C	-29.881.911	-19.649.426	0.0657210
C	-53.207.763	-44.759.550	-0.0880249	C	-16.043.372	-21.163.126	0.0094293
C	-59.967.809	-32.618.252	-0.1249487	C	-0.7970746	-0.9832518	-0.0357708
C	-74.565.501	-30.037.732	0.0556629	H	-32.528.704	14.244.536	0.0467675
C	-39.134.019	-20.988.606	-0.5430071	H	-36.397.933	-28.261.976	0.1016171
C	-32.237.341	-33.052.638	-0.4854193	H	-11.850.810	-31.088.605	-0.0109273
C	-86.348.604	-0.8340025	0.5761109	C	-0.3131960	13.232.410	-0.0355801
C	-53.007.771	-20.627.714	-0.3473070	C	-0.4624923	26.829.497	-0.0691992
C	-82.151.327	-15.128.844	-18.395.199	C	0.6299066	36.016.670	-0.0956327
H	-34.076.843	-54.344.749	-0.2354161	C	-17.333.283	33.332.455	-0.0905215
H	-80.826.994	-36.956.563	-0.5122877	N	14.809.683	43.825.234	-0.1185688
H	-77.259.026	-31.182.526	11.104.197	N	-27.380.894	39.028.802	-0.1085558
H	-95.418.043	-14.394.132	0.6590873	N	-50.089.778	-0.5451850	0.1271938
H	-81.886.934	-0.7574160	15.708.210	N	46.926.681	0.5900201	0.1110374
H	-89.162.390	0.1576524	0.2356992	N	15.951.977	-31.741.757	-0.1284335
H	-83.047.420	-0.4923569	-22.061.286	O	55.777.652	-0.2524562	0.1193440
H	-75.586.920	-20.781.275	-25.063.222	O	48.710.607	17.981.562	0.1485481
H	-92.032.906	-19.802.615	-18.554.073	O	23.686.894	-38.540.193	0.5250061

H	-75.855.370	42.493.620	-0.8340880	O	0.7297068	-36.091.055	-0.8748341
H	-60.660.216	61.977.782	-0.4281042	O	-56.771.825	-15.688.560	0.1582143
H	-36.813.479	58.280.531	0.0820308	O	-54.678.676	0.5883508	0.1390780
S	-42.020.852	0.9084538	-0.0418569				
H	-58.618.085	-54.011.710	0.0724007				
H	-33.544.896	-12.054.502	-0.7698240				
C	-23.363.285	34.727.398	0.2464123				
C	-14.907.170	34.106.218	-0.8739880				
C	-18.090.946	33.660.650	15.445.211				
C	-0.1198337	32.754.890	-0.6747262				
C	-0.4299666	32.387.789	17.008.531				
C	0.4394928	32.060.128	0.6046562				
H	0.5197727	32.200.496	-15.454.118				
H	-0.0320160	31.947.342	27.064.461				
C	-17.449.289	-33.085.819	-0.6582203				
C	-11.709.949	-28.789.246	-18.688.571				
C	-0.9116430	-37.009.226	0.4077975				
C	0.2165930	-28.221.586	-19.808.673				
C	0.4689221	-36.286.939	0.2538469				
C	10.674.558	-31.754.564	-0.9279398				
H	0.6274544	-24.883.506	-29.237.440				
H	10.796.544	-39.188.676	10.970.176				
C	25.420.659	-30.303.827	-10.443.055				
C	33.700.011	-32.696.890	0.0595541				
C	31.365.578	-26.028.246	-22.366.078				
C	47.473.470	-30.826.371	-0.0277949				
H	29.806.087	-35.999.627	10.101.613				
C	45.128.379	-23.995.561	-23.129.416				
H	25.622.994	-24.028.390	-31.283.226				
C	53.405.518	-26.355.249	-12.105.976				
H	64.025.336	-24.609.834	-12.663.890				
C	19.103.933	31.221.689	0.7878147				
C	27.744.561	35.472.349	-0.2237869				
C	24.600.854	26.316.338	19.799.722				
C	41.578.742	34.839.016	-0.0512529				
H	24.053.682	39.506.780	-11.555.001				
C	38.412.520	26.130.367	21.622.910				
H	18.389.808	22.645.996	27.840.169				
C	47.096.660	30.320.250	11.499.710				
H	57.773.472	29.820.880	12.867.878				
C	-20.490.409	34.680.407	-22.732.379				
H	-26.486.426	43.678.651	-24.306.498				
H	-12.472.459	34.561.754	-30.120.199				
H	-26.954.091	26.087.007	-24.692.933				
C	-27.167.528	33.761.573	27.462.709				
H	-33.482.113	42.684.384	27.648.048				
H	-33.764.793	25.043.463	27.173.583				

H	-21.384.780	33.455.648	36.704.974
C	-20.139.180	-24.735.752	-30.545.157
H	-29.225.888	-30.723.827	-31.272.573
H	-23.132.440	-14.242.326	-29.847.244
H	-14.468.272	-25.866.600	-39.793.426
C	-14.776.583	-41.652.643	17.282.874
H	-22.985.178	-35.284.484	20.622.714
H	-18.694.569	-51.837.787	16.624.456
H	-0.7030253	-41.630.175	24.964.138
O	48.990.001	38.704.347	-11.238.452
O	49.683.798	-19.211.933	-35.036.989
O	54.397.419	-33.156.061	11.218.001
O	42.736.075	21.095.920	33.523.530
C	68.668.942	-33.603.736	10.594.056
H	72.826.093	-23.770.144	0.8270057
H	71.937.374	-36.628.130	20.517.006
H	71.990.003	-40.949.460	0.3204429
C	56.140.853	23.916.633	37.666.545
H	56.903.950	20.133.038	47.834.589
H	63.444.771	18.808.905	31.355.933
H	58.005.906	34.688.183	37.556.718
C	63.801.857	-18.640.277	-37.223.901
H	65.022.001	-15.244.948	-47.483.333
H	68.539.383	-11.462.373	-30.486.390
H	68.337.612	-28.516.342	-36.022.294
C	63.215.423	39.068.251	-0.9920954
H	67.238.339	29.103.024	-0.7959985
H	66.946.549	42.597.772	-19.505.020
H	66.230.977	45.986.412	-0.2004810
O	-39.421.480	0.5905832	14.278.273
C	25.248.100	0.7823592	-27.197.300
C	37.897.639	0.8037577	-21.738.681
C	40.368.434	0.4199659	-0.8613054
C	29.554.868	0.0718062	-0.0736566
C	16.130.882	0.1251251	-0.5577508
C	14.419.079	0.4348898	-19.138.371
H	23.747.073	10.175.986	-37.610.793
H	50.510.792	0.3996120	-0.5051974
C	15.440.071	-0.6398530	16.567.990
C	0.9804481	-10.988.725	28.367.254
C	-0.4086612	-11.284.153	29.160.353
C	-12.306.906	-0.6839931	18.930.931
C	-0.6584146	-0.2436887	0.7018340
C	0.7232162	-0.2580683	0.5553812
H	15.635.674	-14.223.725	36.829.124
H	-23.050.086	-0.6467086	20.104.647
H	-12.927.724	0.1224767	-0.0816844

C	29.521.709	-0.4219012	13.121.905
C	40.416.875	-0.6210514	21.153.621
C	39.565.704	-11.421.332	34.356.014
C	53.722.702	-0.3223131	17.172.577
N	39.279.445	-15.690.792	45.087.023
N	64.638.284	-0.0661049	14.365.490
N	49.230.476	11.885.404	-30.204.550
O	60.452.026	11.134.326	-25.279.507
O	46.912.115	15.585.225	-41.614.413
N	0.1566446	0.3577223	-26.295.934
O	0.2040144	0.1280715	-38.316.953
O	-0.8816232	0.5266388	-20.084.893
N	-10.251.633	-16.476.081	41.497.914
O	-22.469.113	-16.564.538	42.188.175
O	-0.2789184	-20.540.382	50.331.606

References

1. Wiedbrauk, S.; Bartelmann, T.; Thumser, S.; Mayer, P.; Dube, H., *Nat. Commun.* **2018**, *9* (1), 1456.
2. <http://supramolecular.org>.
3. Brynn Hibbert, D.; Thordarson, P., *Chem. Commun.* **2016**, *52* (87), 12792-12805.
4. Frisch, M. J.; Trucks, G. W.; Schlegel, H. B.; Scuseria, G. E.; Robb, M. A.; Cheeseman, J. R.; Scalmani, G.; Barone, V.; Petersson, G. A.; Nakatsuji, H.; Li, X.; Caricato, M.; Marenich, A. V.; Bloino, J.; Janesko, B. G.; Gomperts, R.; Mennucci, B.; Hratchian, H. P.; Ortiz, J. V.; Izmaylov, A. F.; Sonnenberg, J. L.; Williams; Ding, F.; Lipparini, F.; Egidi, F.; Goings, J.; Peng, B.; Petrone, A.; Henderson, T.; Ranasinghe, D.; Zakrzewski, V. G.; Gao, J.; Rega, N.; Zheng, G.; Liang, W.; Hada, M.; Ehara, M.; Toyota, K.; Fukuda, R.; Hasegawa, J.; Ishida, M.; Nakajima, T.; Honda, Y.; Kitao, O.; Nakai, H.; Vreven, T.; Throssell, K.; Montgomery Jr., J. A.; Peralta, J. E.; Ogliaro, F.; Bearpark, M. J.; Heyd, J. J.; Brothers, E. N.; Kudin, K. N.; Staroverov, V. N.; Keith, T. A.; Kobayashi, R.; Normand, J.; Raghavachari, K.; Rendell, A. P.; Burant, J. C.; Iyengar, S. S.; Tomasi, J.; Cossi, M.; Millam, J. M.; Klene, M.; Adamo, C.; Cammi, R.; Ochterski, J. W.; Martin, R. L.; Morokuma, K.; Farkas, O.; Foresman, J. B.; Fox, D. J. *Gaussian 16 Rev. C.01*, Wallingford, CT, 2016.
5. Grimme, S., *Chem. Eur. J.* **2012**, *18* (32), 9955-9964.
6. Bruker (2012). SAINT. Bruker AXS Inc., Madison, Wisconsin, USA.
7. Sheldrick, G. M. (1996). SADABS. University of Göttingen, Germany.
8. Sheldrick, G. M., *Acta Cryst.* **2015**, *A71*, 3-8.
9. Spek, A. L., *Acta Cryst.* **2015**, *C71*, 9-18.
10. Farrugia, L. J., *J. Appl. Cryst.* **2012**, *45*, 849-854.